Available online at www.sciencedirect.com
SCIENCE DIRECT®
Journal of Computational Physics 191 (2003) 97–129
JOURNAL OF COMPUTATIONAL PHYSICS
www.elsevier.com/locate/jcp

An "attachment kinetics-based" volume of fraction method for organic crystallization: a fluid-dynamic approach to macromolecular-crystal engineering

Marcello Lappa *

MARS (Microgravity Advanced Research and Support Center) Via Gianturco 31, Napoli 80146, Italy

Received 9 October 2002; received in revised form 14 May 2003; accepted 2 June 2003

Abstract

This analysis exhibits a strong interdisciplinary nature and deals with advances in protein (crystal) engineering models and computational methods as well as with novel results on the relative importance of 'controlling forces' in macromolecular crystal growth. The attention is focused in particular on microgravity fluid-dynamic aspects. From a numerical point of view, the growing crystal gives rise to a moving boundary problem. A 'kinetic-coefficient-based' volume tracking method is specifically and carefully developed according to the complex properties and mechanisms of macromolecular protein crystal growth taking into account the possibility of anisotropic (faceted) surface-orientation-dependent growth. The method is used to shed some light on the interplay of surface attachment kinetics and mass transport (diffusive or convective) in liquid phase and on several mechanisms still poorly understood. It is shown that the size of a growing crystal plays a 'critical role' in the relative importance of surface effects and in determining the intensity of convection. Convective effects, in turn, are found to impact growth rates, macroscopic structures of precipitates, particle size and morphology as well as the mechanisms driving growth. The paper introduces a novel computational method (that simulates the growth due to the slow addition of solute molecules to a lattice and can handle the shape of organic growing crystals under the influence of natural convection) and, at the same time, represents a quite exhaustive attempt to help organic crystal growers to discern the complex interrelations among the various parameters under one's control (that are not independent of one another) and to elaborate rational guidelines relating to physical factors that can influence the probability of success in crystallizing protein substances.

1. Introduction

In the last years great interest has been directed towards crystals of biological macromolecules and towards the crystallization process of protein substances. In fact, single crystals with good diffraction

* Corresponding author. Fax: +39-81-6042100.
E-mail addresses: marlappa@marscenter.it, marlappa@unina.it (M. Lappa).

0021-9991/$ - see front matter © 2003 Elsevier Science B.V. All rights reserved.
doi:10.1016/S0021-9991(03)00307-3

properties and structural quality are needed to achieve high resolution data on protein structure, needed for progress in biotech and drug. Typically, the crystals are obtained by precipitation from super-saturated solutions with a number of techniques. Producing protein crystals of adequate size, however, is often the 'bottleneck' for three-dimensional, atomic-resolution structure studies of protein molecules. Superimposed on this is the poor state of our current understanding of macromolecular crystallization mechanisms and the forces that promote and maintain these mechanisms. For this reason, further investigation is required.

Because of the large size and complexity of protein molecules and the weakness of the bonding forces between them, it is often believed that the experimental principles and methodologies (and associated mathematical models) underlying high-quality inorganic crystal growth are of little help in protein crystallization.

Macromolecules are extremely complex physical–chemical systems whose properties vary as a function of many environmental influences. Moreover, the various parameters under one's control are not independent of one another and their interrelations may be difficult to discern. It is, therefore, not easy to elaborate rational guidelines relating to physical factors that can increase the probability of success in crystallizing a particular protein.

Several studies have shown that the growth rates are sensitive to a very large amount of parameters, e.g., temperature, supersaturation, defect formation, shear forces, etc. In particular, it has been shown that the growth rates can be crystal surface-orientation dependent, i.e., that the different faces of a growing crystal may exhibit different growth according to the crystallographic structure ('faceted' or anisotropic growth; see, e.g. [1]); correspondingly crystal 'habit' change may occur due to changes in the level of supersaturation. The problem is very complex and far to be well understood. An exhaustive review of the previous fundamental protein crystal growth and morphology experimental studies has been given in Monaco and Rosenberger [2] and in Vekilov and Chernov [3]. These reviews show in particular that previous experimental reports have offered conflicting results on the 'controlling forces' in protein crystal growth.

With regard to the rate of growth of protein crystals, it is well known that there are two important effects to consider: the transport of molecules to the face of a growing nucleus or crystal, and the frequency with which the molecules orient and attach themselves to the growing surface (i.e., crystal growth rates can be considered in terms of mass transport in liquid phase and attachment kinetics). However, the results provided by the different investigators do not agree about the relative importance of these two effects. The presence of a distinct boundary layer about the crystals supports the idea of competitive transport and attachment kinetics in limiting the crystal growth rate. However, the interplay between these effects is still unknown even if the case of mass transport in liquid phase simply governed by diffusion is considered. Superimposed on this is the poor state of our current understanding of the effect of convective transport in liquid phase. Some interesting information has been provided by recent experiments in space.

Crystallization experiments carried out in microgravity conditions, in fact, have yielded protein crystals that resulted in diffraction data of significantly higher resolution than the best crystals of these proteins grown on Earth. Since an obvious difference between the space and Earth-based experiments is the magnitude of the buoyancy forces in the solution, the role of solutal convection in protein crystal growth has been proved to be very important.

Protein crystals are typically grown from solutions that, in addition to the solvent and protein, contain a precipitant of well-defined bulk concentration. The interactions between these species in the solution are not well understood. Neither is how convection affects these interactions. In general convection enhances mass transport. As a consequence, crystal growth rates in most inorganic systems are increased by convection. Some experimental results obtained in the case of protein substances suggest that convection seems to influence interface behaviour. Convective effects in protein precipitation processes however are very poorly understood. It is known that they impact protein structures in precipitates, particle size and morphology, but the mechanisms are still unknown. The available experimental results are fragmentary, incomplete and often contradictory (e.g. [4] have found a decrease of the growth rates due to convection).

While efficient numerical methods have been developed and made available for the scientific community in the case of growth of inorganic substances (in particular for the case of crystals grown by thermal solidification of melts under pure diffusive regime or under buoyancy effects), the modelling of the growth of protein crystals and of the interplay between the growth and the presence of convective fields is still an open task.

An interesting effort to the understanding of the interaction between organic crystal growth and convection has been given by Lin et al. [5]. They devised an excellent comprehensive model of convective–diffusive transport in protein crystal growth at standard and zero gravity conditions. Time-dependent solutions were obtained for the convective velocity field, concentration distributions of the protein and precipitant in the solution, the growth rate and salt distribution in the crystal. The protein concentration at the crystal interface was computed using a kinetic-coefficient-based surface condition. The increase of mass (size) of the growing crystal due to protein depletion in the liquid phase however was not taken into account.

According to different experimental studies (see, e.g. [6]), on the other hand, it seems that the increasing size of a growing crystal plays a 'critical role' in the phenomena under investigation and in particular in determining the relative importance of surface attachment kinetics and mass transport in liquid phase under diffusive or convective conditions.

From a numerical point of view, strictly speaking, the growing crystal gives rise to a moving boundary problem. Moving boundary problems are still a challenging task for numerical simulation, have instigated much research, and have led to many different solutions.

A very interesting and pioneer study related to the interplay between crystal growth and convection and to the associate moving boundary problem has been carried out recently by Noh et al. [7]. They investigated the growth behaviours of a precipitate particle in a supersaturated solution under the effect of 'a priori' (well defined) imposed 'ambient' flows. The particle was assumed to have initially a spherical shape. The Stokes flow approximation was assumed to simplify the model. Numerical solutions were obtained through numerically generated orthogonal curvilinear co-ordinate system, automatically adjusted to fit the boundary shape at any instant. Crystal growth rate were computed through consideration of the isotropic and anisotropic interfacial free energies. The initially spherical particle was found to evolve into a peach-like shape if posed in a uniform streaming flow.

Coriell et al. [1] investigated the effect of a parallel shear flow and anisotropic interface kinetics on the onset of morphological instability during growth from a supersaturated solution. Their excellent linear stability analysis was carried out taking into account a kinetic coefficient which is non-linear function of the supersaturation and crystallographic orientation.

The first method capable of modelling complex multi-phase flow separated by a moving interface and capable to undertake a fixed-grid solution without resorting to mathematical manipulations and transformations (i.e., moving grid boundary-fitted methodology), was the Marker and Cell (MAC) of Harlow and Welch [8]. Instead of MAC, however, volume tracking methods (e.g., volume of fluid, SLIC simple line interface calculation, and PLIC piecewise linear interface calculation), front tracking and level-set methods have became popular in the last years (for a very comprehensive discussion dealing with the genesis and the evolution of these methods see the excellent Rider and Kothe [9] and references therein, Hirt and Nichols [10], Osher and Sethian [11], Brackbill et al. [12], Unverdi and Tryggvason [13], Sussman, Smereka and Osher [14], Gueyffier et al. [15], Osher and Fedkiw [16], and Sethian [17]). In particular, they have enjoyed widespread use for the simulation of typical problems associated to gas/liquid or liquid/liquid systems where the surface tension effects play a 'critical role' in determining the shape of the fluid/fluid interface and/or its motion (e.g., gas-bubble or drops in liquid matrices [18,19]; Bassano [20] in particular investigated the thermo-solutal-capillary migration of a liquid drop, injected in a closed cavity filled of a (initially) pure miscible liquid, and the related dissolution process).

On the other hand, 'enthalpy methods' and similar techniques taking into account the release or absorption of latent heat have been successfully applied to the case of thermal phase change problems

characterized by the presence of moving solid/melt interfaces due to the heating or the cooling of the system under investigation. These techniques were pioneered by Voller and Prakash [21], Bennon and Incropera [22,23], Brent et al. [24] and have been strongly improved over the years (see, e.g. [25–30] and many others).

The methodology and the formalism underlying modern volume tracking and level set methods has been extended also to the above-mentioned techniques dealing with the solidification of melts (see, e.g. [31–34]). A tremendous effort on the subject in particular has been provided by Kothe and his co-workers [31,32]. They elaborated a new casting simulation tool (known as ''Telluride'') that employs robust, high-resolution finite volume algorithms for incompressible fluid flow, volume tracking of interfaces, and solidification physics on 3-D unstructured meshes. It can accurately track the topologically complex free surfaces present during mold filling. Coupled to this flow algorithm the authors developed a comprehensive binary alloy solidification model that incorporates macroscopic descriptions of heat transfer, solute redistribution, and melt convection, as well as a microscopic description of segregation.

Despite these worthy and ambitious contributions, however, a complete numerical method aimed at the ('moving boundary') simulation of the growth of organic crystals (due to the addition of solute molecules at the solid/liquid interface) by solubility modulation is still missing.

Macromolecular crystallization is a matter of searching, as systematically as possible, the ranges of the individual parameters that impact upon crystal formation, finding a set or multiple sets of these factors that yield some kind of crystals, and then optimizing the variable sets to obtain the best possible crystals for X-ray analysis.

Aim of the present paper is: (1) to introduce a mathematical model to handle the complex phenomena related to the growth or resolution of protein crystals according to the protein concentration and solubility distribution in the feeding solution, taking into account the mass variation of the crystal due to the incorporation of nutrients and the possibility of (faceted) surface-orientation-dependent growth; (2) shed some light on the complex interplay and relative importance of the surface attachment kinetics and the mass transport (diffusive and/or convective) in liquid phase. In addition to the previous mathematical modelling, the present paper deals in fact with a novel numerical technique to investigate the combined effect of crystal growth and gravitational convection and in particular the interaction of this motion with the concentration field around the crystal and with the growth rates. No simplifying assumptions (such as Stokes flow, 'a priori' imposed ambient flows or 'fixed' crystal size) are assumed in the development of the model.

The present contribution appears as the first attempt to analyze in detail these behaviours.

2. Organic crystal growth

An extensive body of theory and experimental results is available for the crystal growth rate analysis of low molecular weight species. There is less experimental data for higher molecular weight material and in particular for the crystallization of proteins. Factors such as limited availability of material and fragility of the crystals have all combined to limit investigations into protein crystal growth kinetics.

The perplexing difficulties that arise in the crystallization of macromolecules in comparison with conventional small molecules stem from the greater complexity, lability and dynamic properties of proteins. Proteins are very sensitive to their environment and if exposed to sufficiently severe conditions may denature and/or degrade. They must be constantly maintained in a thoroughly hydrated state at or near physiological pH and temperature. Thus common methods for the crystallization of conventional molecules such as evaporation of solvent, dramatic temperature variation, or addition of strong organic solvents are unsuitable and destructive [35,36]. They must be supplanted with more gentle and restricted techniques. Because proteins are sensitive and labile macromolecules that readily loose their native structures, the only conditions that can support crystal growth are those that cause little or no perturbation of the molecular

properties. The protein crystals must be grown from a solution to which they are tolerant. This is called the mother liquor. Because complete hydration is essential for the maintenance of structure, protein crystals are always bathed in the mother liquor.

The strategy employed to bring about crystallization is to guide the system very slowly toward a state of reduced solubility by modifying the properties of the solvent.

The classical procedure for inducing proteins to separate from solution and produce a solid phase is to gradually increase the level of saturation of a precipitant agent.

Protein precipitants fall into four broad categories: (a) salts; (b) organic solvents; (c) long chain polymers and (d) low-molecular-mass polymers and non-volatile organic compounds.

Salts exert their effect by dehydrating proteins through competition for water molecules (their ability to do this being proportional to the square of the valences of the ionic species composing the salt).

For a specific protein, the precipitation point (or solubility minima), however, is usually critically dependent on the pH, temperature, the chemical composition of the precipitant and the properties of both the protein and the solvent. Just as proteins may be driven from solution at constant pH and temperature by the addition or removal of salt, they can similarly be crystallized or precipitated at constant ionic strength by changes in pH or temperature. This is because the electrostatic character of the macromolecule, its surface features, or its conformation may change as a function of pH, temperature and other variables as well.

By these techniques a 'suitable' limited degree of supersaturation can be achieved. In very concentrated solutions, in fact, the macromolecules may aggregate as an amorphous precipitate. This result is to be avoided if possible and is indicative that supersaturation has proceeded too extensively or too swiftly.

Many other distinguishing marks exist with respect to the crystallization of inorganic substances (see, e.g. [37]). In many protein crystallization systems, interfacial kinetics are slow and are considered a major source of difficulties in crystal growth. In many inorganic crystal growth systems, however, the growth rate is limited by the transport of species to the interface so that the fluid-dynamics of the nutrient phase is at the root of growth problems. The inorganic crystal growth in general is not plagued by problems related to interfacial kinetics.

Superimposed on this is the fact that the rate of growth is determined by the nature of the growing crystal surface. Addition of molecules to a rough surface requires less energy than addition to a smooth surface, where surface nucleation is required for addition.

According to the Periodic Bond Chain Theory, [38], three different types of growth faces exist: flat faces, stepped faces and kinked faces. Flat faces require two-dimensional nucleation (the formation of growing sheets of molecules) in order to induce growth, and thus grow the slowest. Stepped faces grow as columns of molecules, which requires only one-dimensional nucleation, and thus have intermediate growth rates. Stepped faces typically occur as a result of a crystallographic screw axis causing spiral growth patterns to occur at the surface of the crystal. Finally kinked faces are growth sites which do not require nucleation to promote further growth, and therefore grow faster than the other two face types. Thus the type of the growing crystal face (flat, stepped, or kinked) strongly influences the rate at which crystal growth occurs (for mathematical models dealing with these aspects see Section 4.1).

In protein crystallization, the problem is further complicated by the incorporation of solvent (water) and solution (also containing precipitant) into the crystal. Thus, in contrast to anhydrous inorganic crystallization, there is only partial (often negligible) rejection of the solvent at the crystal–solution interface.

3. Moving boundary method

In the present paragraph, ancient 'moving boundary' numerical methods and in particular possible novel strategies are briefly outlined in order to point out analogies, similarities and difference with the

sophisticated numerical algorithm proposed here for the case of crystallization of organic substances due to solubility modulation (OCGVOF – organic crystal growth volume of fraction method).

The numerical simulations of these problems require a discretization or nodalization to allow numerical treatment on computers. There are two fundamentally different approaches: Eulerian methods use a frame of reference (discretization grid or mesh, control volumes, etc.) fixed in space, and matter moving through this frame of reference. Lagrangian methods instead use a frame of reference (marker particles) fixed to and moving with the matter.

The first method capable of modelling multi-phase flow, separated by a moving interface, was the Marker and Cell (MAC) of Harlow and Welch [8]. This was in fact a combination of an Eulerian solution of the basic flow field, with Lagrangian marker particles attached to one phase to distinguish it from the other phase. While the staggered mesh layout and other features of MAC have become a model for many other Eulerian codes, the marker particles proved to be computationally too expensive and have been rarely used.

In the specific case of mass crystallization from a supersaturated solution and in order to introduce novel numerical techniques, one must generally accomplish at least two things simultaneously: (a) determine the concentration fields of organic substance and precipitant in the liquid phase and (b) determine the position of the interface between the solid and liquid phases. According to the technique used to address (a) and (b), in principle the numerical procedures able to solve these problems can be divided into two groups:

(1) Multiple region solutions utilizing independent equations for each phase and coupling them with appropriate boundary conditions at the crystal/liquid interface. This approach to the problem takes the point of view that the interface separating the bulk phases is a mathematical boundary of zero thickness where interfacial conditions are applied. These interfacial conditions couple to the concentration equations in the bulk and this system of equations and boundary conditions provides a means to address (a) and (b). Difficulties arise when this technique is employed since in this case in the vicinity of the crystallization front (phase change), conditions on mass flux, velocity and solubility evolution have to be accounted for. This effectively rules out the application of a fixed-grid numerical solution, as deforming grids or transformed (body-fitted) co-ordinate systems are required to account for the position of the crystallization front (see, e.g. [7]).

(2) Single region (continuum) formulations (or 'phase field' models) which eliminate the need for separate equations in each phase, by establishing conservation equations which are universally valid. From a theoretical point of view the major advantage of the single region formulations is that they do not require the use of quasi-steady approximations, numerical remeshing and co-ordinate mapping.

In a phase-field model, a phase-field variable ϕ which varies in space and time is introduced to characterize the phase of the material. In place of the 'sharp' transition from crystal to liquid phases that would characterize the multiple region formulations, here the phase-field varies smoothly but rapidly through an interfacial region. Additionally, in place of the interfacial jump conditions used in the multiple description a differential equation applied over the entire computational domain governs the evolution of ϕ. The effect is a formulation of the free boundary problem that does not require the explicit application of interfacial conditions at the unknown location of a phase boundary. For this reason in the present paper this strategy is adopted.

4. OCGVOF – organic crystal growth volume of fraction method

4.1. General properties

The OCGVOF method, which, similarly to volume tracking and enthalpy methods, is a single region formulation, allows a fixed-grid solution to be undertaken and is therefore able to utilize standard solution procedures for the fluid flow and species equations directly, without resorting to mathematical manipulations and transformations.

This method accounts for the solid mass stored in the generic computational cell by assigning an appropriate value of ϕ to each mesh point ($\phi = 1$ crystal, $\phi = 0$ feeding solution and $0 < \phi < 1$ for an interfacial cell). The key element for the OCGVOF method is its technique for adjourning ϕ. Upon changing phase, the ϕ-value of the cell is adjusted to account for mass release or absorption, this adjustment being reflected in the protein concentration distribution as either a source or sink. The modelling of these phenomena leads to the introduction of a group of differential equations, strictly related, from a mathematical point of view, to the 'kinetic conditions' used to model mass transfer at the crystal surface.

On a molecular level crystal growth consists of the successive addition of 'growth units' or 'building blocks' (nutrients) to a lattice. Growth units can consist of single molecules or possibly of clusters of molecules. In solution, growth units are typically solvated, i.e., are surrounded by highly regularly arranged shells of solvent molecules that interact with the growth unit in a bond-like fashion. Protein crystallization does not fit any of the traditional (inorganic) models without major modification. Realistic models for protein growth kinetics will have to accommodate that protein crystals consist of (see, e.g. [37]):

(a) Protein molecules on regular lattice sites forming a mesh-like network; (b) 'bound water' that lines the large channels formed by the wide-open protein network in bond-like arrangements that are regular enough to be identified by X-ray diffraction and (c) 'bulk water'.

These complicating features make it very unlikely that protein growth kinetics will follow any unmodified inorganic growth models. Hence not surprisingly, the few available results for protein growth rate dependence on bulk supersaturation deviate in form as well as magnitude considerably from any inorganic model predictions.

The 'attachment rates' in protein crystallization are considerably lower than in most inorganic systems (this slow interface kinetics has been interpreted in terms of the low symmetry and the small binding energies involved in protein crystallization).

Because of these theoretical difficulties, Pusey et al. [6] expressed the growth rate of a protein substance as an 'empirical function' of supersaturation introducing a 'kinetic coefficient' ([cm s^{-1}]) dependent on the physical properties of the protein.

This model is adopted in the present paper and further improved to take into account anisotropic growth. This situation occurs for crystalline proteins which have high anisotropy (preferred orientations) in either their surface energy or atomic attachment kinetics.

Surface attachment kinetics at the crystal surface depend on the local value of solubility and on a coefficient λ (kinetic coefficient) having the dimension of a velocity whose value may be different according to the local orientation of the crystal surface (surface-orientation-dependent growth); using mass balance (see, e.g. [37]), and assuming a linear dependence of the growth rate by the interface supersaturation (see, e.g. [5]), one obtains:

$$\left(\frac{D}{\rho_P - \rho_C C_i/\rho_S}\right)\left.\frac{\partial C}{\partial n}\right|_i = \lambda\left(\underline{\hat{n}}\right)\left(\frac{C_i - S}{S} - \delta_0\right), \tag{1}$$

where C_i is the concentration of the protein at the crystal surface, D is the related diffusion coefficient, S is the solubility (its value is function of the local concentration of the precipitant agent and/or of temperature), ρ_P and ρ_C are the protein mass density and the total mass density in the crystal, ρ_S is the total density of the solution, δ_0 is the width of the supersaturation zone in which no growth occurs, $\lambda(\underline{\hat{n}})$ is the kinetic coefficient and $\underline{\hat{n}}$ is the unit vector perpendicular to the crystal surface pointing into the liquid. The parameter δ_0 takes into account the so-called 'dead zone', that according to many investigators, in the case of organic substances, is due to the absorption of impurities that lead to strong retardation of the growth kinetics. In the case of protein substances, such 'impurities' are not necessarily extrinsic contaminants, being often the result of protein 'microheterogeneity' [2].

Whenever protein in solute phase and solid crystal co-exist in equilibrium (saturation condition):

$$C_i = S. \tag{2}$$

In a saturated solution, two states exist in equilibrium, the solid phase, and one consisting of molecules free in solution. At saturation, no net increase in the proportion of solid phase can accrue since it would be counterbalanced by an equivalent dissolution. Thus 'crystals do not grow from a saturated solution'. The system must be in a non-equilibrium, or supersaturated state to provide the thermodynamic driving force for crystallization [35].

Solution must by some means be transformed or brought into the supersaturation state whereby its return to equilibrium, forces exclusion of solute molecules into the solid state, the crystal. As long as $C_i < S$, more solid material will dissolve if any. If, on the other hand, $C_i > S$, material will condense on any material *already existing* and augment its size. The 'growth regime' may be very complex and non-linear (see, e.g. [39]). Its features depend on several parameters and in particular it is function of the ratio between surface-attachment kinetics (modelled by Eq. (1)) and mass transport in liquid phase (diffusive or convective).

The nucleation of new material is something else and the features of this phenomenon are out the scope of the present work (for theoretical analysis of this phenomenon see the excellent paper of McPherson [35]; for numerical models dealing with the phenomena of protein nucleation, see, e.g., Lappa et al. [40] and Lappa and Castagnolo [41]); the term 'precipitation' refers in fact to the composite phenomenon of nucleation and subsequent growth. Growth can take place at concentrations lower that those needed for nucleation, as long as $C_i > S$. The solution is said to be *supersaturated* when the solute content is greater than S and the degree of supersaturation σ is defined by $\sigma = C/S$.

4.2. Governing field equations

The model is based on the mass balance equations. Therefore, in absence of convection, the diffusion of protein is governed by the equation

$$\frac{\partial C}{\partial t} = \nabla^2 C \quad \text{if } \phi = 0. \tag{3a}$$

The diffusion of the precipitant agent is governed by the equation (it is assumed that precipitant does not precipitate in solid phase):

$$\frac{\partial C_{\text{salt}}}{\partial t} = \frac{D_{\text{salt}}}{D}\nabla^2 C_{\text{salt}} \quad \text{if } \phi = 0. \tag{3b}$$

The non-dimensional form of the equations results from scaling the lengths by a reference distance (L), the time by L^2/D; the initial value of protein and precipitant agent (salt) are $C_{(0)}$ and $C_{\text{salt}(0)}$, respectively. Note that concentrations are not posed in non-dimensional form ([g cm^{-3}]).

In presence of convection, the flow is governed by the continuity, Navier–Stokes and species equations, that in non-dimensional conservative form read:

$$\underline{\nabla}\cdot\underline{V} = 0, \tag{4}$$

$$\frac{\partial \underline{V}}{\partial t} = -\underline{\nabla} p - \underline{\nabla}\cdot[\underline{V}\underline{V}] + Sc\nabla^2\underline{V} + Sc\ Ra\left(\frac{C}{C_{(0)}} - 1\right)\underline{i}_g + \frac{D_{\text{salt}}}{D}Sc\ Ra_{\text{salt}}\left(\frac{C_{\text{salt}}}{C_{\text{salt}(0)}} - 1\right)\underline{i}_g - Sc\frac{1}{\eta}\underline{V}, \tag{5}$$

where v is the kinematic viscosity,

$$Sc = \frac{\upsilon}{D}, \quad Ra = \frac{g\beta_{\text{prot}}C_{(0)}L^3}{vD}, \quad Ra_{\text{salt}} = \frac{g\beta_{\text{salt}}C_{\text{salt}(0)}L^3}{vD_{\text{salt}}}$$

(the Boussinesq approximation is used to model the buoyancy forces, β_{prot} and β_{salt} are the solutal expansion coefficients related to organic substance and salt, respectively);

$$\frac{\partial C}{\partial t} = \left[-\underline{\nabla} \cdot (\underline{V} C) + \nabla^2 C \right] \quad \text{if } \phi = 0, \tag{6}$$

$$\frac{\partial C_{salt}}{\partial t} = \left[-\underline{\nabla} \cdot (\underline{V} C_{salt}) + D_{salt}/D \nabla^2 C_{salt} \right] \quad \text{if } \phi = 0, \tag{7}$$

where V and p are the non-dimensional velocity and pressure. The reference pressure is $\rho_S D^2/L^2$. Note that in case solubility modulation is induced by temperature control, Eq. (7) must be replaced by the energy equation.

Assumptions invoked in the development of equations for this continuum model include: laminar flow, Newtonian behaviour of the phases (this implies that solids, should be treated as highly viscous fluids), constant phase densities (and Boussinesq approximation).

Moreover the solid phase (crystal) is assumed to be non-deforming and free of internal stress, while the multiphase region (region where phase change occurs, i.e., region where the ''growth units'' are added to the pre-existent crystalline structure) is viewed as a porous solid characterized by an isotropic permeability η by analogy with the enthalpy methods (see, e.g. [21–24,29]).

The species Eqs. (6) and (7) are not solved for the domain occupied by solid phase since macromolecular solute and salt cannot diffuse through the lattice; nutrient is ''incorporated'' (attached) at the crystal surface for $0 < \phi < 1$ according to Eq. (1), i.e., the crystal surface behaves as a sink for the protein available in liquid phase.

The rate of absorption for the above-mentioned phenomenon is usually measured by the so-called ''growth rate'' θ^* (that can be seen also as a measure of the velocity of the moving solid/liquid interface, see the next section for further details).

An important problem with fixed-grid solution procedures, however is accommodating the zero velocity condition, which is required as a liquid region turns to solid. Various methods can be used in principle to 'switch off' velocities in computational cells that are becoming solid (or 'switch on' velocities in the reverse case). Velocities may simply be set to zero. Another possible approach is based on the viscosity. The viscosity of a cell is driven to a very large value as the solid mass stored in this cell increases. The increasing viscosity provides the necessary coupling between the physical state of the material in the cell and the momentum equations, thereby driving velocities to zero in cells that are solid. A third possible approach (porosity approach) requires that computational cells that are undergoing a phase change are modelled as a pseudo-porous media, with the pseudo-permeability η being a function of ϕ ranging between 0 (fully liquid cell) and 1 (fully solid cell). For the present case of macromolecular organic crystal growth, this assumption is based directly on the fact that solid formation occurs as a 'permeable' crystalline matrix which coexists with the liquid phase. The term $-ScV/\eta$ in Eq. (5) is the Darcy term added to the momentum equation to eliminate convection in the solid phase. In the present analysis pseudo-permeability is assumed to vary according to the Carman–Kozeny equation [23,24]).

$$\eta = \frac{(1-\phi+\varepsilon)^3}{(\phi+\varepsilon)^2}, \quad \varepsilon = 10^{-5}. \tag{8}$$

In the pure solid ($\phi = 1$) and pure liquid ($\phi = 0$), Eq. (8) reduces to the appropriate limits, namely $\eta \cong 0$ and $\eta \to \infty$, respectively. In practice the effect of η is as follows: in full liquid elements $1/\eta$ is very small and has no influence; in elements that are changing phase, the value of $1/\eta$ will dominate over the transient, convective and diffusive components of the momentum equation, thereby forcing them to imitate Carman–Kozeny law; in totally solid elements, the final large value of $1/\eta$ will swamp out all terms in the governing equations and force any velocity predictions effectively to zero.

Since the momentum equation is valid throughout the entire domain, explicit consideration need not be given to boundaries between solid, multiphase and liquid regions.

4.3. Phase field equation

On the surface of the crystal ($|\underline{\nabla}\phi| \neq 0,\ 0 < \phi < 1$), protein concentration must satisfy the kinetic condition that in non-dimensional form reads:

$$\left(\frac{1}{\rho_{\mathrm{P}} - \rho_{\mathrm{C}} C_i/\rho_{\mathrm{S}}}\right)\left.\frac{\partial C}{\partial n}\right|_i = \tilde{\lambda}\left(\underline{\hat{n}}\right)(\sigma_i - 1 - \delta_0), \tag{9}$$

where $\tilde{\lambda} = \lambda L/D$, σ is function of the local precipitant concentration and

$$\underline{\hat{n}} = -\frac{\underline{\nabla}\phi}{|\underline{\nabla}\phi|} = (\alpha, \beta), \tag{10}$$

$$\alpha = -\frac{\partial\phi}{\partial x}\Big/\sqrt{\left(\frac{\partial\phi}{\partial x}\right)^2 + \left(\frac{\partial\phi}{\partial y}\right)^2}, \qquad \beta = -\frac{\partial\phi}{\partial y}\Big/\sqrt{\left(\frac{\partial\phi}{\partial x}\right)^2 + \left(\frac{\partial\phi}{\partial y}\right)^2} \tag{11}$$

since $\frac{\partial C}{\partial n} = \alpha\frac{\partial C}{\partial x} + \beta\frac{\partial C}{\partial y}$ (hereafter the subscript 'i' is omitted) Eq. (9) can be written as

$$\alpha\frac{\partial C}{\partial x} + \beta\frac{\partial C}{\partial y} = \tilde{\lambda}(\alpha, \beta)(\rho_{\mathrm{P}} - \rho_{\mathrm{C}} C/\rho_{\mathrm{S}})(C/S - 1 - \delta_0), \tag{12}$$

$\tilde{\lambda}(\rho_{\mathrm{P}} - \rho_{\mathrm{C}} C/\rho_{\mathrm{S}})(C/S - 1 - \delta_0)$ represents the mass exchange flux between solid and liquid phase (i.e., crystal and protein solution). The mass stored in computational cells that are undergoing phase change can be computed according to the equation:

$$\frac{\partial M}{\partial t} = \frac{\lambda(\alpha, \beta)L^4}{D}(\rho_{\mathrm{P}} - \rho_{\mathrm{C}} C/\rho_{\mathrm{S}})(C/S - 1 - \delta_0)\,\mathrm{d}s, \tag{13}$$

where ds is the 'reconstructed' portion of the crystal surface (by definition perpendicular to the interface normal vector $\underline{\hat{n}}$) 'bounded' by the frontier of the control volume (computational cell) located astride the crystal surface.

The non-dimensional volume of the crystal mass stored in a grid cell can be computed as (ρ_{P} is the protein mass density in the crystal):

$$\mathrm{d}v|_{\mathrm{stored}} = \frac{1}{L^3}\frac{M}{\rho_{\mathrm{P}}} \tag{14}$$

correspondingly:

$$\phi = \frac{\mathrm{d}v|_{\mathrm{stored}}}{\mathrm{d}v}, \tag{15}$$

where dv is the volume of the computational cell.

Therefore the phase field equation reads

$$\frac{\partial\phi}{\partial t} = 0 \quad \text{if } |\underline{\nabla}\phi| = 0, \tag{16a}$$

$$\frac{\partial\phi}{\partial t} = \frac{\tilde{\lambda}(\alpha, \beta)(\rho_{\mathrm{P}} - \rho_{\mathrm{C}} C/\rho_{\mathrm{S}})(C/S - 1 - \delta_0)\,\mathrm{d}s}{\rho_{\mathrm{P}}\mathrm{d}v} \quad \text{if } |\underline{\nabla}\phi| \neq 0,\ 0 < \phi < 1 \tag{16b}$$

with C satisfying Eq. (12).

From mass balance the solution for the normal velocity at the interface is:

$$\underline{V}\cdot\hat{\underline{n}} = (\rho_C/\rho_S)\theta^* \quad \text{if } |\underline{\nabla}\phi| \neq 0,\ 0<\phi<1, \tag{17a}$$

where ρ_S (total density of the solution) is computed as $\rho_S = \rho_{H_20}(1+\beta_{prot}C_{(0)}+\beta_{salt}C_{salt(0)})$ and the non-dimensional growth rate (see, e.g. [6]) is computed as:

$$\theta^* = \left(\frac{1}{\rho_P - \rho_C C/\rho_S}\right)\frac{\partial C}{\partial n} = \tilde{\lambda}\left(\hat{\underline{n}}\right)(\sigma - 1 - \delta_0) \tag{17b}$$

with C satisfying Eq. (12).

The parameter θ is a measure of the rate of absorption of the protein at the crystal surface (it is proportional to $\partial C/\partial n$) and can be seen also as a measure of the velocity of the advancing solid/liquid interface. It is called "growth rate" by organic crystal growers and usually is expressed in dimensional form as [Å s^{-1}]. According to the present method it can be computed on the basis of Eq. (17b) after the computation of the protein concentration at the crystal surface according to Eq. (12)).

Eqs. (12), (16), (17a) and (17b) behave as 'moving boundary conditions', their solution being strictly associated to the computational check on the value of ϕ and its gradient. Note that, typically, for organic crystal growth, the normal velocity at the interface is very small with respect to buoyancy induced velocities even if the gravity acceleration is reduced of several orders of magnitude in space, and for this reason it could be neglected with regard to the solution of the momentum equation (for further details on this aspect see the order of magnitude analysis in Section 5.2).

4.4. Discretization

Eqs. (4)–(7) subjected to the initial and boundary conditions are solved numerically in primitive variables by a control volume method. The domain is discretized with a uniform mesh and the flow field variables defined over a staggered grid. Forward differences in time and upwind schemes in space (second order accurate) are used to discretize the partial differential equations, obtaining (n superscript indicates time step):

$$\underline{V}^{n+1} = \underline{V}^n + \Delta t\left[-\underline{\nabla}\cdot(\underline{V}\underline{V}) + Sc\nabla^2\underline{V} + Sc\ Ra\left(\frac{C}{C_{(0)}}-1\right)\underline{i}_g + \frac{D_{salt}}{D}Sc\ Ra_{salt}\left(\frac{C_{salt}}{C_{salt(0)}}-1\right)\underline{i}_g\right]^n - \Delta t\frac{Sc}{\eta}\underline{V}^{n+1} - \Delta t\underline{\nabla}p^n, \tag{18}$$

$$C^{n+1} = C^n + \Delta t\left[-\underline{\nabla}\cdot[\underline{V}C] + \nabla^2 C\right]^n, \tag{19}$$

$$C_{salt}^{n+1} = C_{salt}^n + \Delta t\left[-\underline{\nabla}\cdot[\underline{V}C_{salt}] + \frac{D_{salt}}{D}\nabla^2 C_{salt}\right]^n. \tag{20}$$

The orientation of the surface of the crystal is used in determining the face fluxes for the computation of C at the crystal surface (Eq. (12)). The interface orientation depends on the direction of the volume fraction gradient of the phase within the cell, and that of the neighbour cell (or cells) sharing the face in question.

In practice the unit vector $\hat{\underline{n}}$ results from the gradient of a smoothed phase field $\widehat{\phi}$, where the transition from one phase to the other takes place continuously over several cells. The smoothed phase field $\widehat{\phi}$ is obtained by convolution of the unsmoothed field ϕ with an interpolation function.

Depending on the interface's orientation, concentration gradients are discretized by forward or backward schemes. For this reason Eq. (12) in discretized form reads:

$$\alpha > 0,\ \ \beta > 0: \quad C_{i,j}^{n+1} = \frac{\left[\tilde{\lambda}(1+\delta_0)\left(\rho_P - \rho_C C_{i,j}^{n+1}/\rho_S\right) + \alpha C_{i+1,j}^{n+1}/\Delta x + \beta C_{i,j+1}^{n+1}/\Delta y\right]}{\left[\tilde{\lambda}\left(\rho_P - \rho_C C_{i,j}^{n+1}/\rho_S\right)/S + \alpha/\Delta x + \beta/\Delta y\right]}, \tag{21a}$$

$$\alpha < 0,\ \ \beta > 0: \quad C_{i,j}^{n+1} = \frac{\left[\tilde{\lambda}(1+\delta_0)\left(\rho_P - \rho_C C_{i,j}^{n+1}/\rho_S\right) - \alpha C_{i-1,j}^{n+1}/\Delta x + \beta C_{i,j+1}^{n+1}/\Delta y\right]}{\left[\tilde{\lambda}\left(\rho_P - \rho_C C_{i,j}^{n+1}/\rho_S\right)/S - \alpha/\Delta x + \beta/\Delta y\right]}, \tag{21b}$$

$$\alpha > 0,\ \ \beta < 0: \quad C_{i,j}^{n+1} = \frac{\left[\tilde{\lambda}(1+\delta_0)\left(\rho_P - \rho_C C_{i,j}^{n+1}/\rho_S\right) + \alpha C_{i+1,j}^{n+1}/\Delta x - \beta C_{i,j-1}^{n+1}/\Delta y\right]}{\left[\tilde{\lambda}\left(\rho_P - \rho_C C_{i,j}^{n+1}/\rho_S\right)/S + \alpha/\Delta x - \beta/\Delta y\right]}, \tag{21c}$$

$$\alpha < 0,\ \ \beta < 0: \quad C_{i,j}^{n+1} = \frac{\left[\tilde{\lambda}(1+\delta_0)\left(\rho_P - \rho_C C_{i,j}^{n+1}/\rho_S\right) - \alpha C_{i-1,j}^{n+1}/\Delta x - \beta C_{i,j-1}^{n+1}/\Delta y\right]}{\left[\tilde{\lambda}\left(\rho_P - \rho_C C_{i,j}^{n+1}/\rho_S\right)/S - \alpha/\Delta x - \beta/\Delta y\right]}, \tag{21d}$$

$C_{i,j}^{n+1}$ is computed from Eq. (21a)–(21d) iterating up to reach convergence, then the phase variable is updated using Eq. (16):

$$\phi_{i,j}^{n+1} = \phi_{i,j}^{n} + \Delta t \frac{\tilde{\lambda}\left(\rho_P - \rho_C C_{i,j}^{n+1}/\rho_S\right)(C_{i,j}^{n+1}/S - 1 - \delta_0)\Delta s}{\rho_P \Delta x \Delta y}. \tag{22}$$

According to Eqs. (21a)–(21d) and (22), if the protein concentration is locally depleted, correspondingly, the solid mass stored in the computational cell grows and the phase variable is increased; on the other hand if mass stored in the cell begins to re-dissolve, protein is released in solute phase and the local value of protein concentration is increased. These phenomena are driven by the attachment kinetic condition, i.e., the existing deposit grows if protein concentration is larger than S and the mass exchange is proportional to the local value of the orientation-dependent kinetic coefficient; in the opposite situation, i.e., in case protein concentration becomes smaller than S, deposit begins to re-dissolve. The solubility is function of the precipitant agent (salt) concentration and for this reason the phenomena are mainly governed by the distribution of this agent (i.e., by Eq. (20), or by temperature in case solubility modulation is induced by thermal control).

In Eq. (22) Δs is the 'reconstructed' portion of the solid wall 'bounded' by the frontier of the control volume (computational cell) located astride the crystal surface. The determination of Δs requires a well defined 'interface-reconstruction' technique (the shape of the crystal for a fixed time is not known a priori and must be determined as part of the solution). A reconstruction is a geometrical approximation of the true solid/liquid interface. Usually the interface can be approximated by a straight line of appropriate inclination in each cell (PLIC piecewise linear interface approximation) and this reconstruction technique is used for the present analysis. Various conditions can be used to determine the reconstruction, one of which is a condition that the straight lines connect at cell-faces. With this condition, the resulting interface representation becomes continuous. However, for strong distortions and topology changes similar to those involved in organic crystal growth, this conditions becomes virtually unenforceable. If non-connecting straight lines (each line is determined independently of the neighbour lines and their ends need not necessarily connect at the cell-faces, see, e.g., Gueyffier et al. [15] and the PLIC method) are used, this guarantees maximum robustness and simplicity, and allows extension to three dimensions, while sacrificing little in accuracy.

Two conditions can be used for the straight line in cell (i,j), which always yield an unambiguous solution: (a) it is perpendicular to the interface-normal-unit vector $\underline{\hat{n}}$ and (b) it delimits a solid area 'matching' the given $\phi^n_{i,j}$ for the cell; i.e., the slope of the line is given by the interface normal (gradient of the volume fractions), and the intercept follows from invoking volume conservation.

The reconstructed interface is then used to compute the fluxes (i.e., for the present case the mass flux of "growth units" that are incorporated by the crystal) necessary to integrate the volume evolution equations.

The computation of the velocity field at each time step is split into two substeps.

In the first, an approximate non-solenoidal velocity field $\underline{V}^*$ which corresponds to the correct vorticity of the field is computed at time $(n+1)$ neglecting the pressure gradient term in the momentum Eq. (18). In the second substep, the pressure field is computed by solving the equation resulting from the divergence of the momentum equation taking into account Eq. (4):

$$\nabla^2 p^n = \frac{1}{\Delta t}\underline{\nabla}\cdot\underline{V}^*. \tag{23}$$

This equation is solved with a SOR (Successive Over Relaxation) iterative method. For further details on the numerical method, see, e.g., Monti et al. [42] and Savino et al. [43]. On the solid walls the $\partial P/\partial n = 0$ condition is imposed; at the crystal surface, this condition is discretized by forward or backward schemes according to the interface's orientation:

$$0<\phi<1,\ \ \alpha>0,\ \ \beta>0: \qquad P_{i,j}=\frac{\left(\alpha P_{i+1,j}/\Delta x+\beta P_{i,j+1}/\Delta y\right)}{(\alpha/\Delta x+\beta/\Delta y)}, \tag{24a}$$

$$0<\phi<1,\ \ \alpha<0,\ \ \beta>0: \qquad P_{i,j}=\frac{\left(-\alpha P_{i-1,j}/\Delta x+\beta P_{i,j+1}/\Delta y\right)}{(-\alpha/\Delta x+\beta/\Delta y)}, \tag{24b}$$

$$0<\phi<1,\ \ \alpha>0,\ \ \beta<0: \qquad P_{i,j}=\frac{\left(\alpha P_{i+1,j}/\Delta x-\beta P_{i,j-1}/\Delta y\right)}{(\alpha/\Delta x-\beta/\Delta y)}, \tag{24c}$$

$$0<\phi<1,\ \ \alpha<0,\ \ \beta<0: \qquad P_{i,j}=\frac{\left(-\alpha P_{i-1,j}/\Delta x-\beta P_{i,j-1}/\Delta y\right)}{(-\alpha/\Delta x-\beta/\Delta y)}. \tag{24d}$$

Finally, the correct solenoidal velocity field is updated using the computed pressure field to account for continuity:

$$\underline{V}^{n+1}=\underline{V}^*-\Delta t\underline{\nabla}p^n. \tag{25}$$

The protein and salt distributions at time $(n+1)$ are obtained from Eqs. (19) and (20) after the velocity calculation.

Parallel supercalculus is used due to the enormous time required for the computations. Calculations dealing with the behaviour of melts and/or phase change problems in fact often are very heavy (see, e.g. [31,32,44]. Superimposed on this is the fact that in the case of macromolecular crystallization it is necessary to simulate very long times (the time required for the growth of protein crystals, in fact, is quite variable and may range from a few hours in the best of cases to several months in others). The problem is split in two problems, one parabolic and the other elliptic. A parallel algorithm, explicit in time, is utilized to solve the parabolic equations (momentum and species equations). A parallel multisplitting kernel is introduced for the solution of the pseudo-pressure elliptic equation, representing the most time-consuming part of the algorithm. A grid-partition strategy is used in the parallel implementations of both the parabolic equations and the multisplitting elliptic kernel. A Message Passing Interface (MPI) is coded for interprocessor communications. For the sake

of brevity the parallel implementation of the OCGVOF method is not described in detail. For further details on parallel strategies, see, e.g., Lappa [45] and Lappa and Savino [46].

4.5. Validation

The code has been validated through comparison with the numerical results of Lin et al. [5]. They investigated the time-dependent diffusive–convective transport in an isothermal protein crystal growth system at standard gravity. A rectangular crystal of dimensions 400 [μm] × 600 [μm] was positioned at the bottom of a 1 [mm] high and 6 [mm] wide growth cell.

Since the increase of crystal volume during the five hours simulation was assumed to be negligible with respect to the overall cell dimensions, a 'fixed crystal' size was assumed in the numerical computations. The same conditions have been simulated with the OCGVOF. A uniform grid of 300 × 100 points has been used in order to achieve high accuracy.

The present results show good agreement with the results of Lin et al. [5] (see, e.g., Fig. 1(a) to be compared with Figs. 4(b) and 7(b) in the paper of Lin et al. [5]). The maximum velocity and the corner

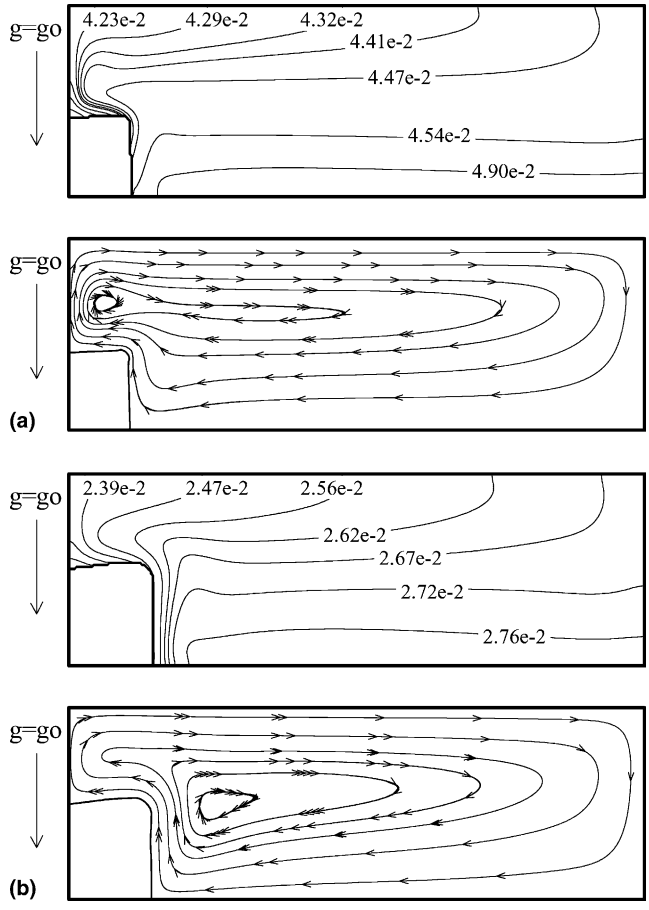

Fig. 1. Comparison with the numerical results of Lin et al. [5]: isothermal protein crystal growth system under normal gravity conditions (rectangular lysozyme crystal of initial dimensions 400 [μm] × 600 [μm] positioned at the bottom of a 1 [mm] high and 6 [mm] wide growth cell). Protein concentration distribution [g cm^{-3}] and velocity field: (a) $t = 1$ [h], (b) $t = 4$ [h].

growth rate at $t = 18\,000$ [s] are 8.1×10^{-4} [cm s^{-1}] and 41 [Å s^{-1}] in good agreement with the values obtained by Lin et al. [5] (8.6×10^{-4} [cm s^{-1}] and 44 [Å s^{-1}], respectively). The small difference between the present results and those obtained by Lin et al. [5] could be explained according to the fact that during the five hours simulations the crystal undergoes small dimensional changes (Fig. 1(b)) that were not taken into account in the model of Lin et al. [5] and/or by the fact that a very dense mesh has been used for the present simulations. Further validation, moreover, has been provided through comparison with experimental results (see Section 5.1).

4.6. Discussion

The volume tracking and enthalpy methods, become so popular in the last years, are single region formulations. In the present paragraph, the OCGVOF method is briefly compared with these methods with which it shares some features. Moreover the applicability of the method is discussed.

Volume of fluid methods do not use marker particles. The liquid volume-fraction field ϕ, is used. It indicates for each computational cell its liquid fraction (e.g., $\phi = 1$ liquid, $\phi = 0$, gas and $0 < \phi < 1$ for an interfacial cell). The key element for a volume of fluid method is its technique for advecting ϕ: standard finite-difference methods suffer from numerical diffusion, which would soon smooth ϕ excessively. The ϕ-field is the only phase information stored in volume of fluid methods. Approximate interface locations are found from a so-called interface reconstruction. This is needed for 'advecting' ϕ (a transport equation is solved at each time step to determine the relative position of the different phases, i.e., the ϕ-distribution), for determining the local properties of the fluid (e.g., viscosity) and for better graphical representation.

In a phase-field model for the thermal solidification of a liquid ('enthalpy method'), similarly to the case of volume of fluid methods, a phase-field variable ϕ which varies in space and time is introduced to characterize the phase of the material. Contrary to the case of volume of fluid methods, however, in this case the phase-field variable ϕ is not 'advected' by the motion of the fluid, but computed as function of the temperature distribution. An energy partial differential equation applied throughout the computational domain and taking into account the release or absorption of latent heat associated to the phase change, governs the evolution of ϕ.

In the volume of fluid methods, ϕ is 'advected' solving an appropriate continuity transport (i.e. volume tracking) equation, in the enthalpy methods ϕ is computed as function of the temperature obtained solving an appropriate energy equation taking into account the release or absorption of latent heat, in the OCGVOF method, ϕ is computed using attachment kinetics at the surface of the crystal i.e. it is computed taking into account the phenomenon of addition/incorporation of solute molecules (building blocks or growth units) to the crystal. These conditions lead to the introduction of a group of differential equations for the protein concentration at the crystal surface and the evolution of the solid mass displacement.

The OCGVOF technique shares with the aforementioned classical methods the interface orientation analysis, that in these methods is needed to compute the surface tension force perpendicular to the interface separating the fluid-phases (expressed as a corresponding volume force, which can be included in the momentum equation), whereas in the OCGVOF method it is needed for the orientation-dependent kinetic coefficients and the discretization of the protein concentration gradients perpendicular to the surface (fluxes of nutrients). Moreover it shares with the enthalpy methods the technique used to accommodate the zero velocity condition in liquid regions turning to solid phase (the so-called 'mushy' regions). This discussion clarifies the analogies and differences among these methods.

It is also interesting to point out how the ideas and concepts at the root of the OCGVOF technique have led to the introduction of a similar method for the simulation of the growth of organic ''living'' tissues in bioreactors. In this case however the mathematical model is quite different since the living-construct exhibits high sensitivity to the effect of the fluid-dynamic shear stress at the surface (shear-stress dependent kinetics). In the case of macromolecular crystals the growth units are merely ''added'' to the solid (the

molecules orient and attach themselves to the growing surface) without changing their initial composition. In the case of biological tissues of course the mechanism is more complex. The growth units are incorporated and "converted" into the main tissue components. Consequently tissue enlargement occurs due to "internal cell division" and "production of extracellular matrix" supported by the aforementioned incorporation of nutrients in the biological cells. The surface shear stress acts modifying the manner with which absorbed nutrients are used to produce the new cells and the extracellular matrix (it induces changes in the tissue metabolism and function eliciting a physiologic response from the biological cells, see, Lappa [47] for further details on the modelling of these aspects and the related volume tracking method).

Note that, in principle, since constant phase densities are assumed, the OCGVOF method provides reliable results only if the decrease of solution volume due to the advancing interface is negligible. In the case of inorganic crystal growth, since solvent inclusions in the solid mass are very small, this would occur if the decrease of solution volume was only a few per cent of its initial volume (i.e. if the crystal undergoes only small dimensional changes with respect to the overall dimensions of the cell containing the feeding solution). Fortunately this problem is not remarkable for the case of protein substances. Protein crystals, in fact, have widely open structures and incorporate up to 90% by volume of solvent within the network of protein molecules. Macromolecular crystals are mainly composed of solvent. The protein occupies the remaining volume so that the entire crystal is in many ways an ordered gel with extensive interstitial spaces through which solvent and other 'small' molecules may freely diffuse (see, e.g. [35,37]).

5. Results

Hen egg-white lysozyme is used as model protein, being a well-characterized molecule (see Table 1 for the properties). The precipitant agent is NaCl. The tetragonal form of hen egg-white lysozyme typically grows in a habit formed by a combination of prismatic (1 1 0) and pyramidal (1 0 1–0 1 1) faces (see, e.g. [2]).

In order to show the capabilities of the numerical method, its robustness and versatility and how it can deal with very different situations, two 'typical' cases are considered. In the first case, analysis of growth habit change is carried out in the case of micro-crystals having size of the order of 50 [μm] (study of the microscopic facet morphologies) for typical experimental conditions and in absence of convection (diffusive transport). In the second case, the growth of a lysozyme macro-crystal (size 1 [mm]) is investigated under the effect of buoyancy convection induced by typical values of residual gravity occurring on orbiting space platforms (e.g., the Space Shuttle or the International Space Station).

In order to characterize the interplay of surface attachment kinetics and mass transport (diffusive/convective) in liquid phase a non-dimensional parameter is introduced.

Table 1
Properties and operating conditions

D_{lys} [cm^2 s^{-1}]	10^{-6}
D_{NaCl} [cm^2 s^{-1}]	10^{-5}
ν [cm^2 s^{-1}]	8.63×10^{-3}
ρ_C [g cm^{-3}]	1.2
β_{lys} [g^{-1} cm^3]	0.3
β_{NaCl} [g^{-1} cm^3]	0.6
ρ_P [mg ml^{-1}]	820
λ [Å s^{-1}]	$\cong$10
δ_0 [–]	2
T [°C]	18
pH	4.5

If attachment kinetics is the rate-limiting step in the growth process, $C_i = C_B$ (C_B – bulk protein concentration) and the local supersaturation will be approximately the bulk supersaturation. On the other hand, if the growth rate is limited by transport (convective or diffusive) of solute to the growth interface, $C_i = S$. These processes can be characterized by use of a surface coefficient γ defined as

$$\gamma = \frac{(C_B - C_i)}{(C_B - S)} \tag{26}$$

this coefficient is a measure of the relative importance of surface kinetics versus transport as the rate-limiting step in the growth of crystals. For growth controlled by surface kinetics $C_i \to C_B$ and $\gamma \to 0$; for a transport controlled process, $C_i \cong S$ and $\gamma \to 1$.

Transport and surface kinetics processes can be considered competitive for $\gamma \cong 0.3$ to 0.5.

5.1. Growth habit simulation and microscopic facet morphology study

In order to obtain crystals of high compositional uniformity it is important that the growth rate is kept constant over the whole advancing interface, i.e., that the crystal shape remains unchanged during growth. The conditions required for morphological (i.e., shape) stability of interfaces are well understood for the diffusive 'transport-limited' growth of non-faceted crystals (in this case, particle growth is mainly controlled by mass transport to the interface and the growth behaviour depends on the local mass flux at the interface, Rosenberger [37]). There the growth kinetics are rather isotropic and interfacial processes are relatively unimportant for the stability. However most protein crystals, when grown not too rapidly, are faceted and the present paragraph deals with the shape evolution of precipitate particles in this case ('faceted growth').

This implies that the growth kinetics are anisotropic, i.e., that the kinetics of incorporation at the crystal surface are strictly linked to the different crystallographic directions. Then morphological stability is governed by the interaction between the non-uniform interfacial processes and mass transfer to the interface.

The experimental results of Monaco and Rosenberger [2] are considered for comparison.

Monaco and Rosenberger [2] found experimentally that the habits of lysozyme crystallites and larger crystals (up to 500 [μm]) were bound by (1 0 1 or 0 1 1) and (1 1 0) faces (see Fig. 2). This overall habit formed regardless of the supersaturation prevailing during nucleation and growth. However, the aspect ratios of the (1 1 0) faces were found to be dependent on the growth conditions. At low σs, the distance between opposite (1 0 1–0 1 1) pyramids far exceeded the distance between opposite (1 1 0) faces. At high σs,

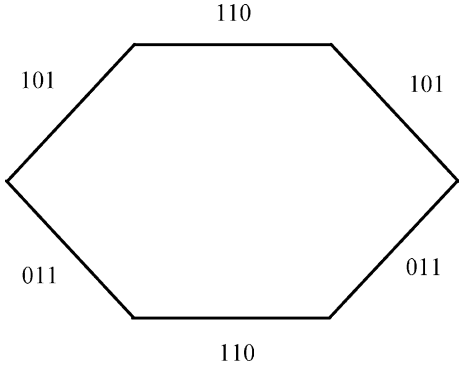

Fig. 2. Tetragonal form of hen egg-white lysozyme typically growing in a habit formed by a combination of prismatic (1 1 0) and pyramidal (1 0 1–0 1 1) faces.

the reverse occurred. They found differences in the average growth rate (θ) of adjacent faces according to the space-orientation of the faces and according to the value of the supersaturation. In particular the macroscopic growth rates were found to be almost equal for $\sigma_{(0)} < 8$ with the (1 1 0) growth rate located below the (1 0 1) one (e.g., $\theta_{1\,0\,1} = \theta_{0\,1\,1} = 1.3\theta_{1\,1\,0}$ for $\sigma_{(0)} = 6$), whereas the opposite situation occurred for $\sigma_{(0)} > 8$ with $\theta_{1\,1\,0}$ far located above $\theta_{1\,0\,1}$ ($\theta_{1\,1\,0} = 1.86\theta_{1\,0\,1}$ for $\sigma_{(0)} = 11$).

According to Monaco and Rosenberger [2], the observed phenomena for $\sigma_{(0)} \leqslant 11$ were controlled mainly by surface attachment kinetics (interface kinetically limited phenomena); therefore it is reasonable to assume that the different behaviour of the differently oriented faces were strictly associated to different values of the kinetic coefficient. In the case of pure kinetically driven situations, the kinetics of incorporation at the crystal surface are strictly linked to the bond configuration of the crystallographic structure whereas other effects are negligible. This is a simplified case of the more general situation that can be handled by the mathematical model presented in Section 4.3.

The numerical results presented in this paragraph have been obtained for two different situations. In the first case ($\sigma_{(0)} = 6$), the kinetic coefficients (in literature this value is affected by a large uncertainty, many investigators found values around 10^{-7} [cm s^{-1}]) $\lambda_{1\,0\,1} = \lambda_{0\,1\,1} \cong 1.5 \times 10^{-7}$ [cm s^{-1}] and $\lambda_{1\,1\,0} = 0.75\lambda_{1\,0\,1}$ are assumed for the different faces of the crystal (this corresponds to Monaco and Rosenberger's $\sigma_{(0)} < 8$ condition). For the second case ($\sigma_{(0)} = 11$), the orientation-dependent crystal growth is simulated by assuming $\lambda_{1\,0\,1} = \lambda_{0\,1\,1} \cong 10^{-7}$ [cm s^{-1}] and $\lambda_{1\,1\,0} = 1.86\lambda_{1\,0\,1}$ (this information being extrapolated from the experimental behaviour of the kinetically limited average growth rates).

In the experiments of Monaco and Rosenberger [2] crystal growth was obtained from a supersaturated solution with $C_{\mathrm{lys}(0)} = 5 \times 10^{-2}$ [g cm^{-3}] and solubility modulation was controlled by temperature. For the present simulations solubility modulation is induced by setting an appropriate salt concentration whose value is supposed to be constant in the bulk liquid phase. The dependence of S of lysozyme on C_{NaCl} has been determined experimentally by other investigators (see, e.g. [48]). Correspondingly the values of C_{NaCl} needed to obtain $\sigma_{(0)} = 6$ and $\sigma_{(0)} = 11$ and used for the present numerical simulations, are $C_{\mathrm{NaCl}(0)} = 2.65 \times 10^{-2}$ [g cm^{-3}] and $C_{\mathrm{NaCl}(0)} = 3.3 \times 10^{-2}$ [g cm^{-3}], respectively. For both the cases a seed crystal having a size of 50 [μm] is placed in the centre of a computational domain having a width of 10^3 [μm] and the concentration of protein is supposed to be constant at the initial time. The frontier of the computational domain is supposed to be impermeable to protein and salt. A grid 200×200 is used to achieve good resolution.

The results, grouped in Fig. 3 ($\sigma_{(0)} = 6$) and Fig. 4 ($\sigma_{(0)} = 11$) show the different growth habit of the crystals according to the value of the supersaturation and according to the corresponding surface kinetic coefficient distribution.

The computed face growth rates versus time are shown in Figs. 3(b) and 4(b). The computed time-averaged growth rates ($\sigma = 6, \theta_{1\,0\,1} \cong 18$ [Å s^{-1}], $\sigma = 11, \theta_{1\,1\,0} \cong 59$ [Å s^{-1}]) are in good agreement with the experimental ones ($\sigma = 6, \theta_{1\,0\,1} \cong 21$ [Å s^{-1}], $\sigma = 11, \theta_{1\,1\,0} \cong 65$ [Å s^{-1}]).

Finally Figs. 3(d) and 4(d) show the time-evolution of the parameter γ. Since $\gamma < 0.2$, these plots confirm the assumption of Monaco and Rosenberger [2] (i.e., that the phenomena under investigation were mainly driven by attachment kinetics) and at the same time provide further validation and justification for the numerical results and the agreement with the experimental ones (in fact, in principle, the relative ratio of the kinetic coefficients for the different faces can be extrapolated from experimental macroscopic averaged growth rates only if the phenomena are kinetically limited). Either experimental observation either numerical modelling exhibit comparable evidences of the phenomena under investigation. Quantitative comparison between experimental observation and numerical simulations provides a validation of the present mathematical model and gives insights on the crystallization process, providing, for instance, evaluation of the kinetic coefficients; the uncertainty related to the value to assign to the kinetic coefficients (in literature located around 10^{-7} [cm s^{-1}]), in fact can be overcome (through OCGVOF) changing these values up to match exactly the macroscopic experimental growth rates.

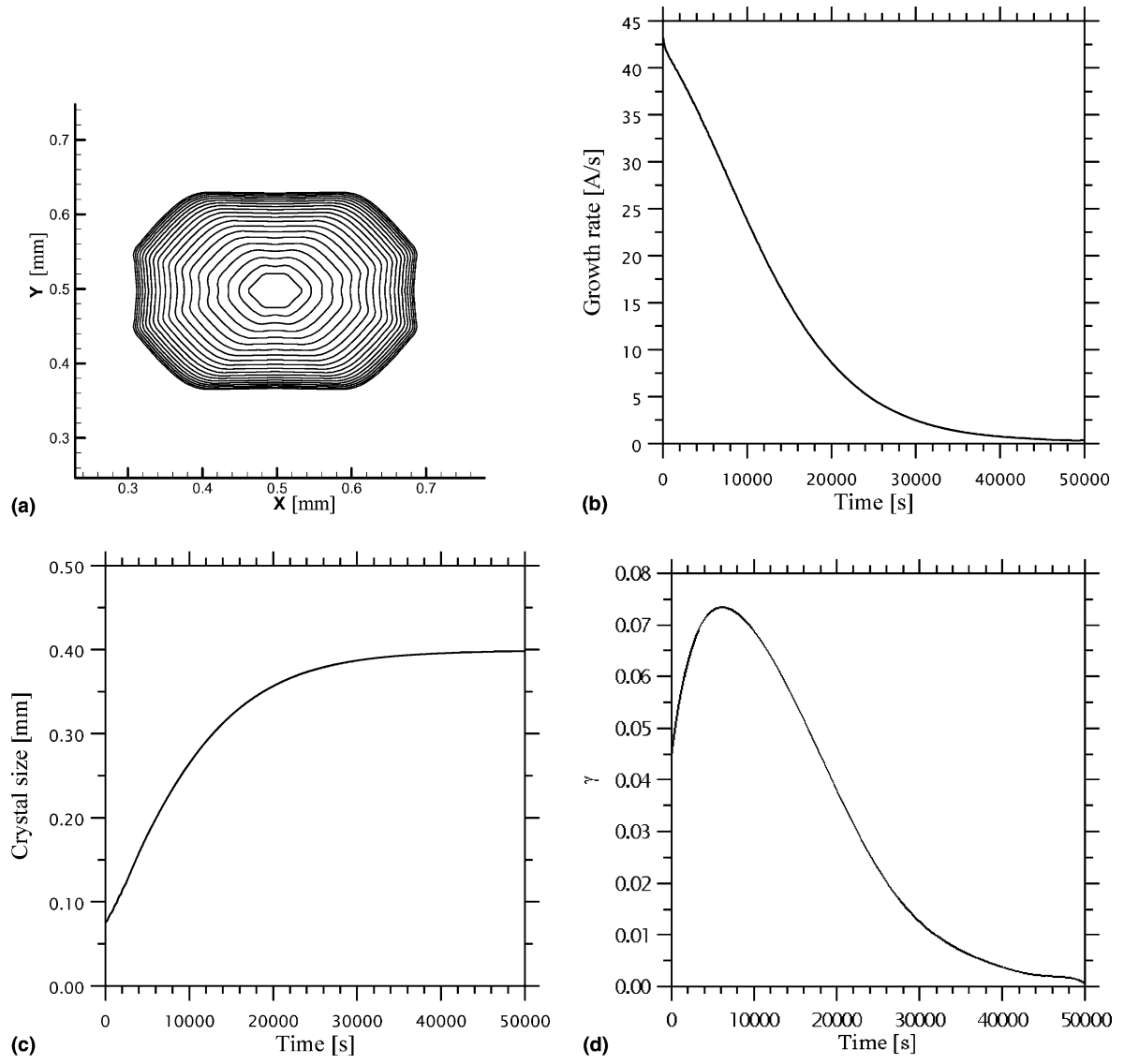

Fig. 3. Growth habit simulation and microscopic facet morphology study of a faceted seed of lysozyme: $C_{\mathrm{lys}(0)} = 5 \times 10^{-2}$ [g cm^{-3}], $C_{\mathrm{NaCl}(0)} = 2.65 \times 10^{-2}$ ($\sigma_{(0)} = 6$), $\lambda_{1\,0\,1} = \lambda_{0\,1\,1} \cong 1.5 \times 10^{-7}$ [cm s^{-1}], $\lambda_{1\,1\,0} = 0.75\lambda_{1\,0\,1}$: (a) snapshots of the crystal shape versus time ($\Delta t = 1220$ [s]); (b) growth rate of the 1 0 1 face versus time; (c) crystal size along $\times$ versus time; (d) γ versus time.

5.2. Macroscopic growth and convective transport

Crystals of biological macromolecules are obtained by precipitation from super-saturated solutions and for this reason crystallization can be influenced by gravity. Concentration (density) gradients exist in the crystallizing solutions (as an intrinsic consequence of the crystal-growth process). The growth process, in fact, depletes of protein the liquid surrounding the growing crystal; the related concentration gradient implies a density gradient that, in presence of gravity, induces buoyancy driven convective flow.

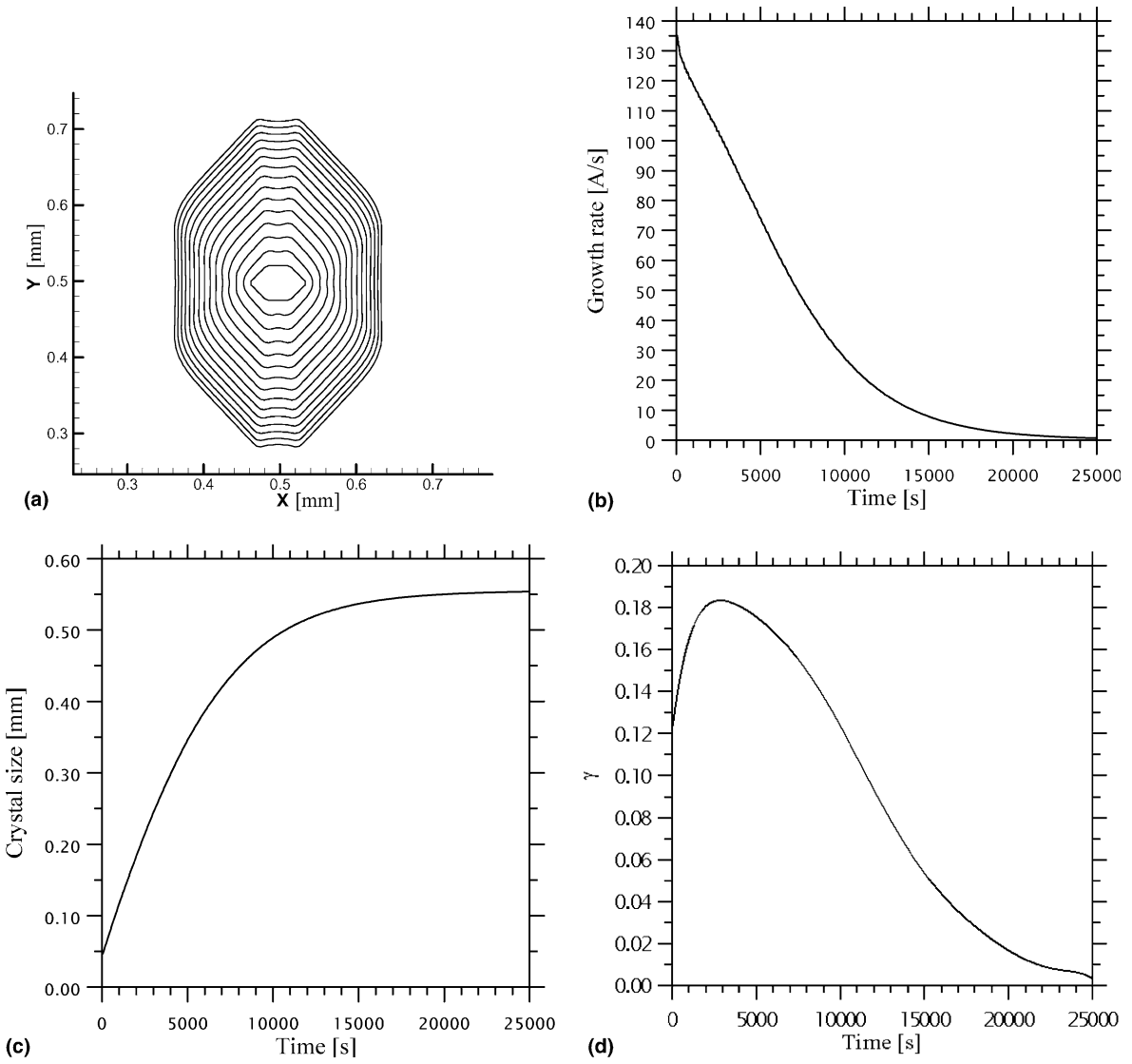

Fig. 4. Growth habit simulation and microscopic facet morphology study of a faceted seed of lysozyme: $C_{\mathrm{lys}(0)} = 5 \times 10^{-2}$ [g cm^{-3}], $C_{\mathrm{NaCl}(0)} = 3.3 \times 10^{-2}$ ($\sigma_{(0)} = 11$), $\lambda_{1\,0\,1} = \lambda_{0\,1\,1} \cong 10^{-7}$ [cm s^{-1}], $\lambda_{1\,1\,0} = 1.86\lambda_{1\,0\,1}$: (a) snapshots of the crystal shape versus time ($\Delta t = 510$ [s]); (b) growth rate of the 1 1 0 face versus time; (c) crystal size along y versus time; (d) γ versus time.

These phenomena occur also during experiments in space. In fact, the residual gravity estimated on board the space-shuttle and the International Space Station (ISS) is not zero, but typically of the order of 10^{-5} of earth gravity. Therefore these effects have to be evaluated also under microgravity conditions, in order to properly prepare and interpret the results of crystal growth experiments in space.

In the present paragraph, the growth of a seed macro-crystal of lysozyme under micro-gravity conditions is simulated. For the sake of simplicity (aim of the present paper is merely to show the capabilities of the numerical method and how it can 'capture' heretofore poorly understood physics and mechanics of the problem under investigation) the initial shape of the seed crystal is supposed to be quadrate and the kinetic

coefficient is supposed to be the same for the different sides of the crystal (however the numerical method can handle complex shapes and surface-orientation-dependent growth as shown in Section 5.1). Moreover though the acceleration environment on the ISS exhibits a rich variation in magnitude and orientation over the course of a mission with a broad range of frequency content, (see, e.g. [49–52]) a residual (steady) $g = 10^{-4} g_0$ (100 [μg]) oriented in a single direction is considered. This is a simplistic and conservative assumption. The detailed investigation of the changing orientation of the quasi-steady component of acceleration, the presence of g-jitters with or without vibration isolation, etc. is out of the scope of the present work and is delayed to forthcoming analyses.

In order to discern the effect of convection with respect to other effects, the same simulation is carried out under pure diffusive regime (i.e., absence of convection).

The crystal (1 [mm] × 1 [mm]) is supposed to be fixed (e.g., by glue) to the mean point of the left wall of the reactor (10 [mm] high and 30 [mm] wide test cell) used for the growth process (see Fig. 5). Growth is obtained from a super-saturated solution with $C_{\mathrm{lys}(0)} = 5 \times 10^{-2}$ [g cm^{-3}] and $C_{\mathrm{NaCl}(0)} = 2.5 \times 10^{-2}$ [g cm^{-3}] ($\sigma_{(0)} \cong 5$). The frontier of the domain is supposed to be impermeable to the protein.

Table 2 shows a grid refinement study carried out to ensure good resolution and grid-independence of the results (grid-independence is achieved for a mesh of 300×100 points).

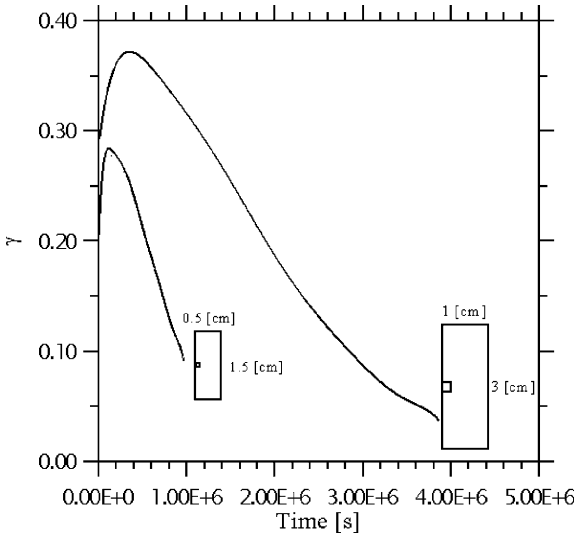

Fig. 5. Effect of the size of the reactor on the non-dimensional parameter γ (diffusive conditions).

Table 2
Grid refinement study (maximum growth rate and maximum velocity as function of the number of grid points at $t = 6.0 \times 10^5$ [s])

Grid	$\theta_{\max}$ [Å s^{-1}]	$V_{\max} \times 10^5$ [cm s^{-1}]
100×33	3.578	2.297
150×50	4.820	3.214
200×75	5.967	4.121
300×100	6.529	4.879
400×130	6.576	4.932

Fig. 5 shows that, since for the case under investigation $\gamma \cong 0.3$ to 0.4, surface attachment kinetics and mass transport in liquid phase can be considered competitive in limiting the growth rate.

Regarding this aspect (that is crucial for the problem under investigation), the same simulation has been repeated halving the dimensions of the system in order to shed some light about the effect of the size of the reactor on the non-dimensional parameter γ. Fig. 5 shows that large systems tend to exhibit transport-dependent (limited) growth rates (γ tends to be high) whereas small systems tend to be governed by surface attachment kinetics (for these systems γ is small; this behaviour is also confirmed by the results described in Section 5.1, see, e.g., Figs. 3(d) and 4(d)).

This trend can be explained according to the fact that, if the dimensions of the system are increased, a high time is required to transport available protein (in solute phase) from far regions (i.e., the frontier of the reactor) towards the crystal surface. This increases the relative importance of mass transport with respect to surface attachment kinetics in limiting the growth rate.

As a crystal grows from the solution, it depletes the concentration of the growth units that are incorporated into the crystal lattice producing a concentration-depleted zone around it. In this region, the solute concentration changes continuously from the concentration at the crystal face to the concentration in the bulk of the solution. The concentration profile in the concentration-depleted zone varies with time as the crystal grows and is controlled by the balance between the flow of growth units towards the crystal face and the rate of incorporation of these growth units into the crystal lattice. The kinetics of incorporation at the crystal surface are linked to the bond configuration of the crystallographic structure as discussed in paragraph 5.1 (for the present case of isotropic growth, the kinetics of incorporation are simply linked to the value of the kinetic coefficient and to the supersaturation level), while the flow towards the crystal face is highly dependent on the mass-transport properties in the bulk solution (diffusive or convective), which turn out to be crucial for the overall crystal-growth process.

In case convection is absent, Fig. 6(b) shows that the face growth rate drops with increasing face size (correspondingly, in Fig. 6(a), the size of the crystal tends to an asymptotic constant value). This behaviour can be explained according to two effects:

(a) the finite volume of the test cell (the amount of solute protein available for the growth of the solid phase is finite and decreases as time passes); (b) as the size of the face increases, more solute should be added to maintain a given face growth rate.

Fig. 6(a) shows deviation from diffusion-controlled growth (which would show a square-root dependence of the crystal size on time). This illustrates the fact that even when diffusive transport is ensured, no guarantee exists that the crystal will grow in the diffusion-controlled regime: the growth regime is a function of the ratio between diffusion transport and surface attachment kinetics.

Figs. 6(c) and (d) show that after a short initial transient, γ decreases. This is due to diffusive transport that decreases in intensity the concentration gradient between the crystal and regions far from its surface (in 'finite size' systems the relative importance of mass transport in liquid phase with respect to surface attachment kinetics decreases as time passes due to the decrease of available protein and related gradients).

The above results refer to macroscopic parameters; from a 'local' point of view, the simulations show that corners and edges of the crystal are more readily supplied with solute than the centre of faces (this leads to a macroscopic depression around the centre of the faces, see Figs. 7(a) and 8). This is due to the diffusive pattern of the protein concentration field around the crystal. Incorporation of the solute into the crystal causes a local depletion in concentration and a solutal concentration gradient to form between the bulk solution and the growth interface. The 'steepness' of the gradient determines the rate of solute transport to the growth interface, the steepness being maximum around the corners. Superimposed on this is the fact that a protuberance on the interface sees a higher supersaturation and grows faster than a depression, which sees a lower supersaturation. Note that the existence of 'depressions' around the centre of the faces of growing crystals (shown by the present numerical results) has been often observed experimentally (Monaco

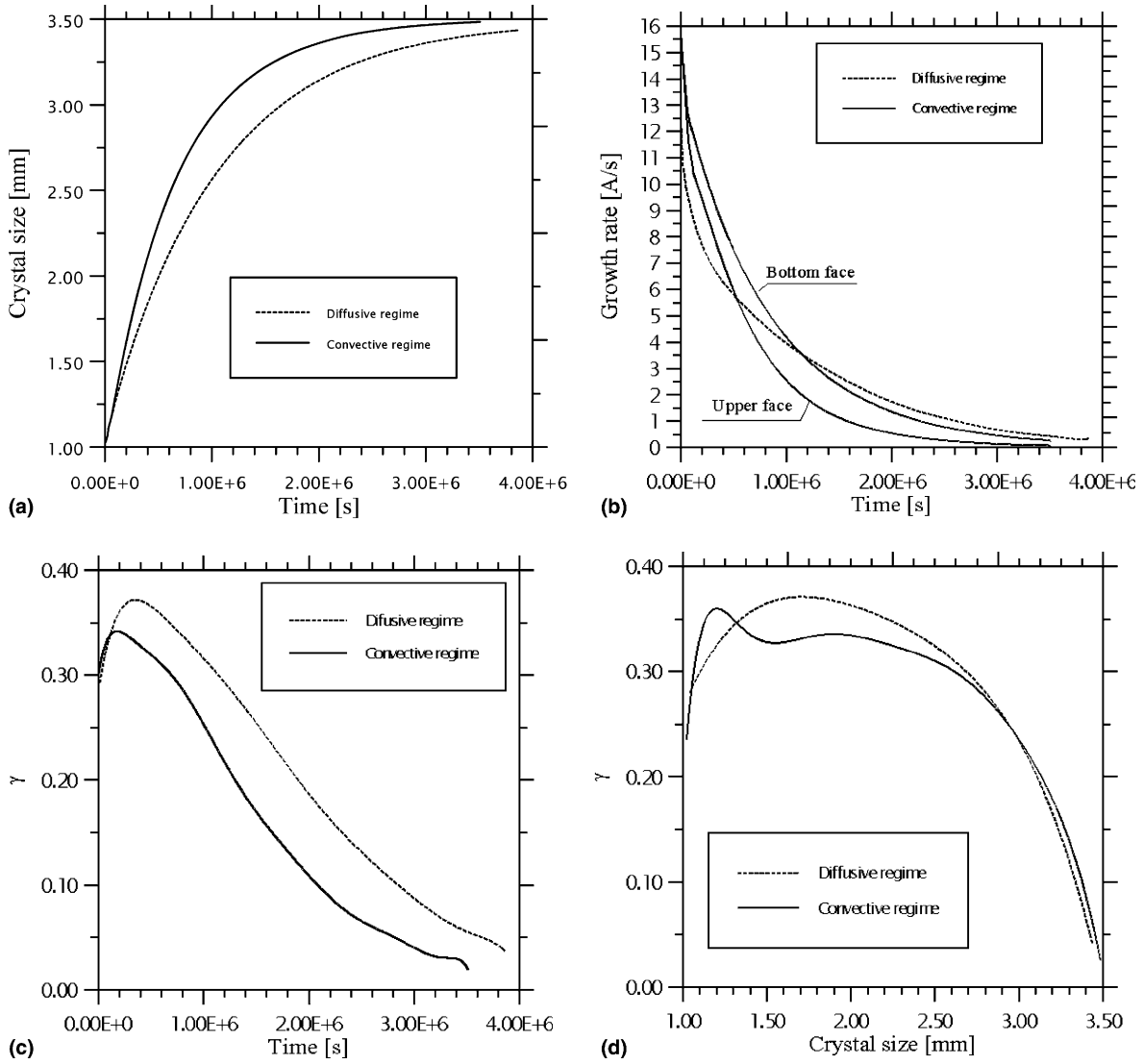

Fig. 6. Isothermal protein crystal growth system under diffusive and microgravity (convective) conditions (crystal of initial dimensions 1 [mm] × 1 [mm] fixed to the left wall of a 3 [cm] high and 1 [cm] wide growth cell; $C_{\mathrm{lys}(0)} = 5 \times 10^{-2}$ [g cm^{-3}] and $C_{\mathrm{NaCl}(0)} = 2.5 \times 10^{-2}$ [g cm^{-3}]): (a) average size (along y) versus time; (b) growth rate versus time; (c) γ versus time; (d) γ versus crystal size.

and Rosenberger [2]). Fig. 7(a) shows that the difference in gradient steepness between face corner and face centre (and consequently the 'depth' of the depressions) is proportional to the size of the crystal.

If the presence of convection is taken into account a flow field is driven by the density gradient around the growing crystal. Since isothermal conditions are assumed throughout the growth process, only compositional non-uniformities, that evolve in the solution due to the crystallization process, act as source for buoyancy-driven convection. This flow field modifies the protein distribution around the crystal leading to a non-symmetrical concentration pattern (Fig. 9). One recognizes the well-known convective flow pattern for solution growth with a rising 'plume' above the crystal. When growth sets in, the solute concentration

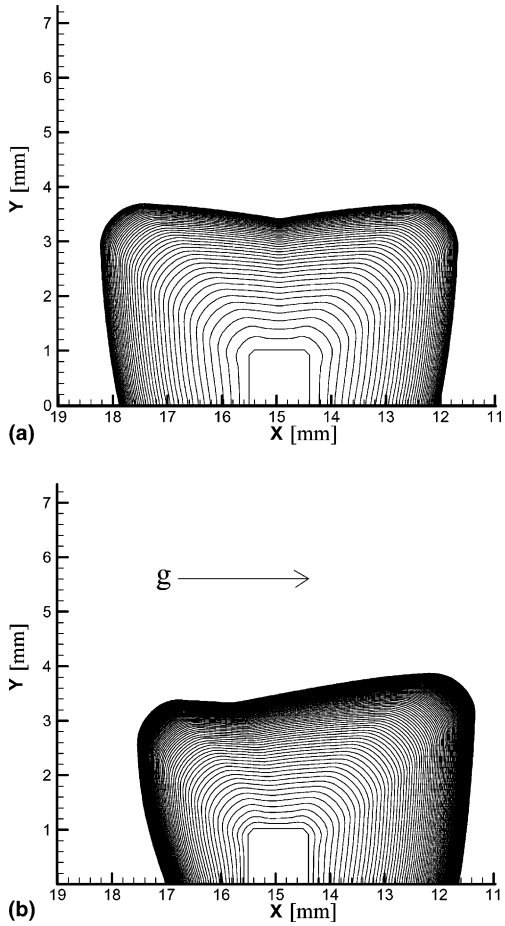

Fig. 7. Growth habit simulation of a seed of lysozyme ($C_{lys(0)} = 5 \times 10^{-2}$ [g cm^{-3}], $C_{NaCl(0)} = 2.5 \times 10^{-2}$): (a) diffusive regime, snapshots of the crystal shape versus time ($\Delta t = 7.7\ 10^4$ [s]), (b) microgravity convective conditions, snapshots of the crystal shape versus time ($\Delta t = 3.5\ 10^4$ [s]).

around the crystal seed decreases. With this depletion of the heavier solute, the solution around the crystal becomes lighter and, thus, rises.

Fig. 9 show that the convective cell however does not extend throughout the bulk of the protein chamber and is confined to the zone between the right face of the growing crystal and the right wall of the test cell. As time passes, the vortex roll shrinks while migrating towards the right wall of the protein chamber (see Fig. 9). The contraction of the cell and its progressive confining to a zone close to the right wall are strictly related to the behaviour of the crystal that puffs out due to growth.

Fig. 6(b) shows that, during the first part of the growth process, the growth rate under the effect of convection is considerably higher than under diffusive conditions. The growth rates decrease with increasing growth time and crystal size (the decrease being more rapid in the diffusion-dominated case). This is due to the effects already pointed out for the case of absence of convection.

The growth rate under the effect of convection is located above the corresponding one obtained under diffusive regime since convection enhances mass transport in liquid phase thus increasing the rate of incorporation of the solute into the crystal.

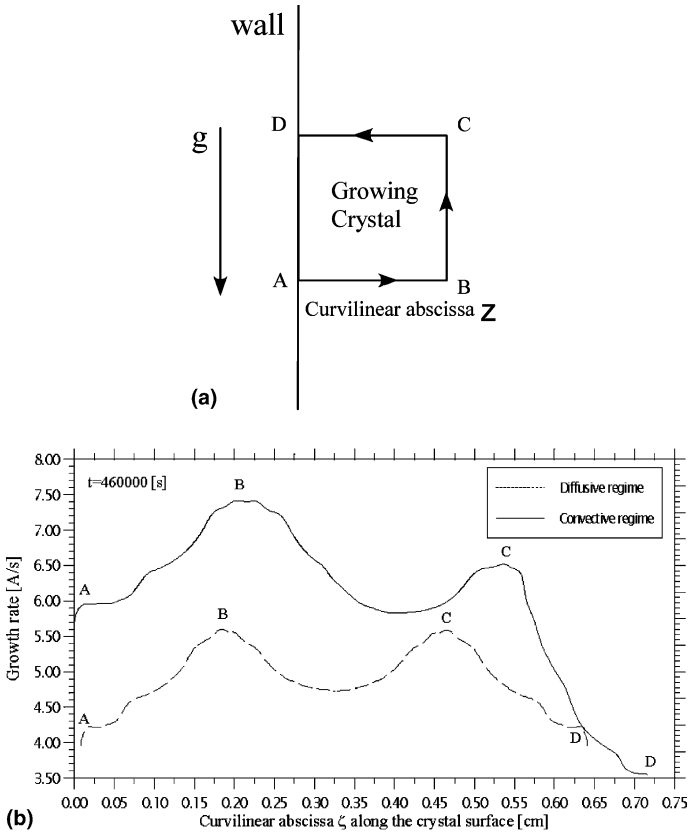

Fig. 8. (a) Curvilinear abscissa along the crystal surface, (b) surface growth rate distribution under diffusive and microgravity (convective) conditions.

In addition to these effects one must keep in mind that there is an effect related to the fact that the magnitude of the flow is directly proportional to the size of the face upon which it is being generated. Thus, as crystal grow, solutal gradient driven flows can become a major factor for the growth rates.

As time passes, however an inversion occurs in the behaviour described above (Fig. 6(b)). The growth rate under diffusive regime becomes higher than the convective ones. This behaviour is strictly related to the 'finite' amount of protein available for the crystal growth (i.e., the 'finite' reactor size). At the beginning the convective growth rate is located above the diffusive one since solute protein is transported towards the crystal surface more rapidly with respect to a pure diffusive situation (convective motion causes fluxes in the bulk of the solution that exceed the mere diffusive ones). Due to this effect, however, the effect of the 'finite' cell size is enhanced.

In the case of reactors having an 'infinite' size, the convective growth rates would be always located above the diffusive ones during the crystal growth process. However if the initial amount of protein available for the growth is finite, this does not happen. This explains why after an initial transient time the diffusive growth rate becomes higher than the convective one and at the same time could explain some contradictory results in literature. Otàlora et al. [4] found a decrease of the growth rates under the effect of convection; this result is in contrast with the generalized idea that convection enhances mass transport in liquid phase increasing the growth rate. According to the present results, this counterintuitive behaviour could be explained by the finite size of their reactor.

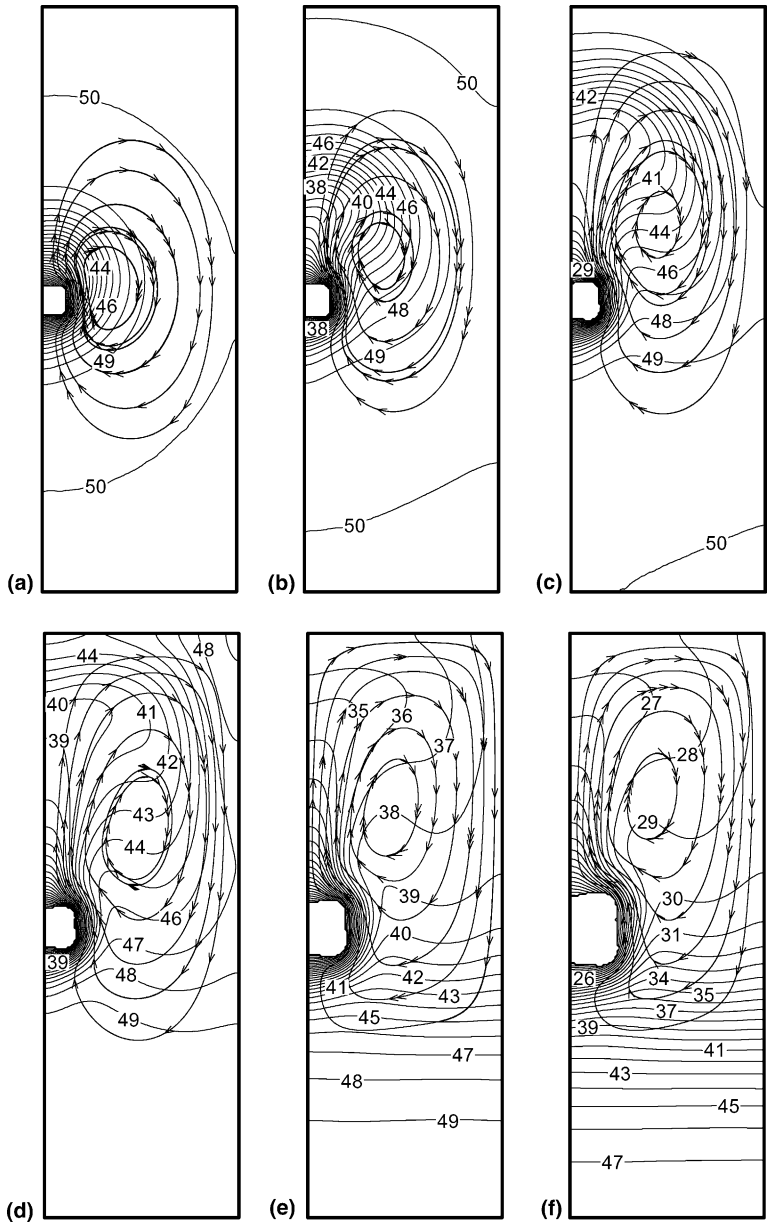

Fig. 9. Snapshots of growing crystal, concentration distribution and velocity field under microgravity conditions ($g = 10^{-4}g_0$): (a) $t = 3.5 \times 10^4$ [s], (b) $t = 7 \times 10^4$ [s], (c) $t = 10.5 \times 10^4$ [s], (d) $t = 14 \times 10^4$ [s], (e) $t = 2.8 \times 10^5$ [s], (f) $t = 4.9 \times 10^5$ [s], (g) $t = 8.75 \times 10^5$ [s], (h) $t = 1.26 \times 10^6$ [s], (i) $t = 1.64 \times 10^6$ [s], (j) $t = 2.0 \times 10^6$ [s], (k) $t = 2.42 \times 10^6$ [s], (l) $t = 2.8 \times 10^6$ [s], (m) $t = 3.19 \times 10^6$ [s], (n) $t = 3.5 \times 10^6$ [s].

Figs. 6(c) and (d) clearly show (as expected) that the parameter γ for the case of convection is located below the corresponding one obtained in the case of diffusive conditions (convection reduces the time required to transport available protein from far regions towards the crystal surface and this decreases the

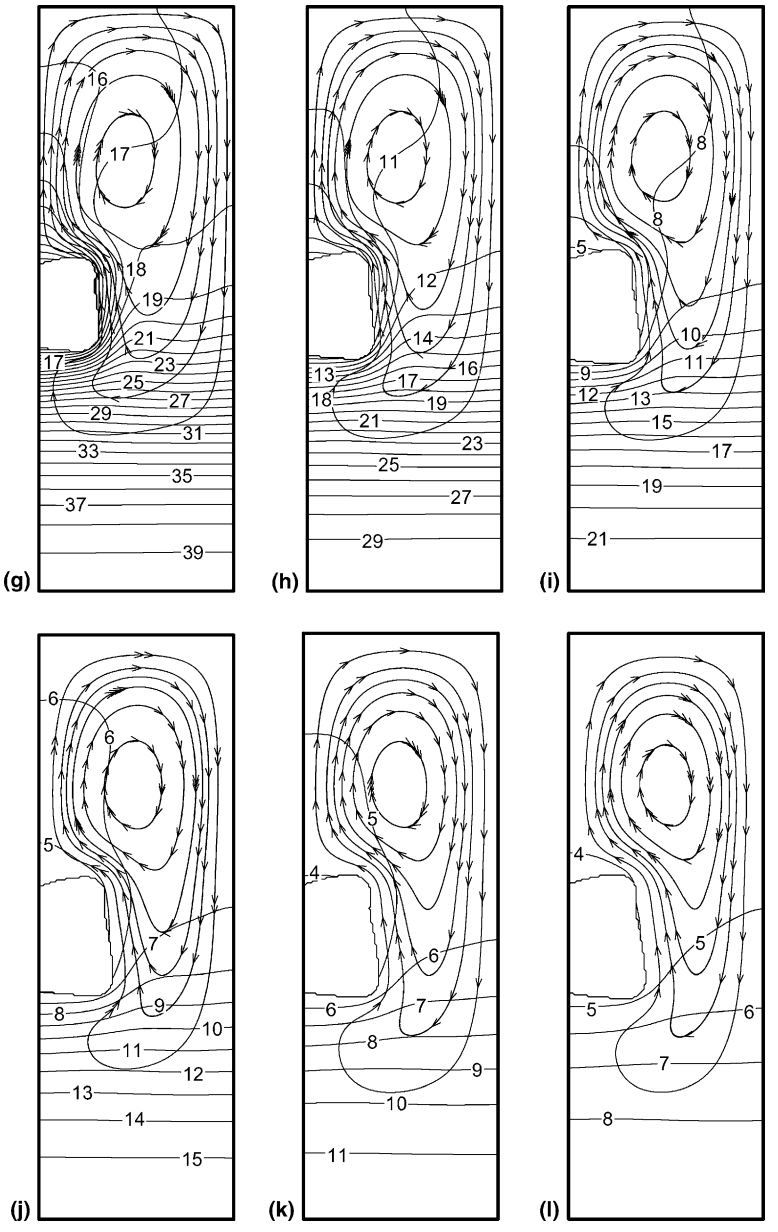

Fig. 9. (*continued*)

relative importance of mass transport with respect to surface attachment kinetics in limiting the growth rate).

Fig. 6(b) shows moreover that the 'face' (average) growth rate exhibits a different value according to the orientation of the face with respect to the direction of the residual g.

This clearly demonstrates that orientation-dependent growth may occur even if the dependence of the kinetic coefficients on the orientation of the faces is neglected. In this case, it is due to the non-symmetrical

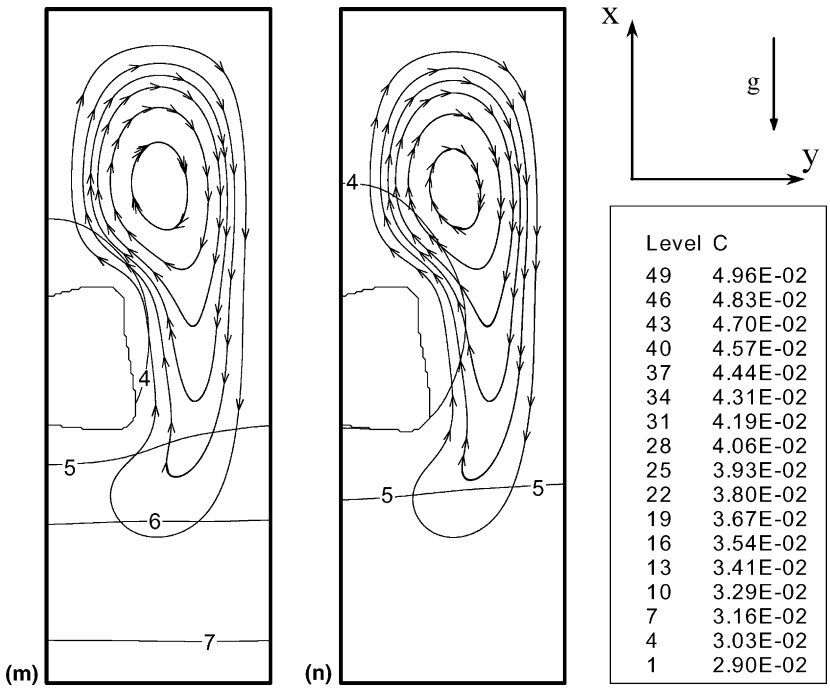

Fig. 9. (*continued*)

concentration pattern around the crystal distorted by the effect of convection according to the direction of the residual g. The growth rate is strongly affected by the mass transport in liquid phase and g-orientation-dependent growth occurs.

Fig. 7(b) shows that the increase of volume of the crystal is more pronounced for the bottom side than for the upper side. Fig. 8 shows in detail how the convection effect results in higher local growth rates near the surface where the flow is incoming and lower local growth rates near the surface where the flow is outgoing. This behaviour can be explained according to two different effects.

Due to the convective structure of the flow pattern, in fact, liquid is transported towards the bottom side and in opposite direction around the upper side. According to this behaviour, liquid regions where the amount of protein available in liquid phase is still large are transported towards the bottom side of the crystal. This increases the growth rate of the lower face (a large amount of protein in solute phase is available for crystal growth). On the other hand, due to the outgoing flow, the depletion zone close to the upper face is distorted and elongated towards the top of the test cell ('plume'). This leads to a decrease of the concentration gradient (the depletion layer becomes thinner with respect to the bottom side of the crystal) and hence to a decrease of the mass exchange flux between solid and liquid phase. This explains the occurrence of a higher value of the growth rate on the bottom face.

The analysis of the surface growth rate distribution in Fig. 8 shows, as for the case of diffusive regime, that the growth rate is non-uniform across the crystal faces. As expected, the growth rate is always lower at the centre than at the corners where the convective flows (and the associated shear stresses) are the strongest, and hence, the interfacial concentration gradients the steepest. However the growth rate distribution is not symmetric and, in particular, the maximum of the growth rate occurs at the corner B. Qualitatively, the predicted higher growth rates at crystal corners are consistent with experimental observations on lysozyme [37].

According to the results described and discussed above, one can speculate that the faster (high supersaturation) a crystal grows the more readily it can lose morphological stability (formation of macroscopic depressions).

The bigger a crystal, the lower may be the critical growth rate for morphological instability.

On the other hand the convective transport in the solution, that also depends on the size of the crystal and/or of the reactor, can influence the growth (morphological stability) behaviour.

For the sake of brevity, however, parametric analyses of the effect of the initial size and position of the seed, of the size of the reactor, of the initial protein concentration, of the initial supersaturation level, of the orientation and intensity of the residual-g, etc. are delayed to forthcoming papers.

At this stage a discussion of the order of magnitudes of the velocity of the moving interface and of the buoyancy-induced velocities in the bulk of the protein reactor can be carried out in order to provide the necessary justification for the assumption of negligible interface velocity in Section 4.3. The order of magnitude of the buoyancy induced-velocity in the bulk is given by: $V_g = g\beta_{\mathrm{lys}}\Delta C L^2/\nu$, where ΔC is the (average) concentration difference between the surface of the crystal and the top (bulk) of the protein chamber (according to the numerical simulations, during the growth process $\Delta C \cong \mathrm{O}(10^{-3})$ [g cm^{-3}], see Fig. 9). Therefore for the present case (see Table 1) $V_g \cong 10^{-1}g$: so in the range of 1 [g] to 1 [μg], the order of magnitude is reduced from $\mathrm{O}(10^{2})$ [cm s^{-1}] to $\mathrm{O}(10^{-4})$ [cm s^{-1}]. On the other hand, the normal velocity at the crystal interface V_n is of the order $\mathrm{O}(10^{-7})$ [cm s^{-1}] (the time required to increase the size from 1 [mm] to 3.5 [mm] is about 3×10^6 [s], see Figs. 6(a) and (b)). Therefore it is very small even if compared to the case 1 [μg]. This provides reliability for the present assumption of $V_n \cong 0$ in the case of 100 [μg].

It is worthwhile to stress how in the specific case of lysozyme, the computational model can be easily further improved by taking into account the incorporation of the precipitant agent in the solid crystal according to the excellent model proposed by Lin et al. [5]. Other simulations can be carried out, moreover, about the case of salt concentration non-constant in the reactor (e.g., salt diffusing in the test cell through a membrane or a agarose gel interface, etc). Furthermore the method can be used to investigate the case of many interacting crystals (usually in fact the growth process is associated to multiple nucleation events; see, e.g. [53–55] and the problem exhibits a high topological complexity) and/or different growth configurations (e.g., drops on depression spot plates and hanging drops) where other types of convection (e.g., Marangoni flow) may influence the growth process.

Second order spatial accuracy and first order temporal accuracy have been achieved for the present computations respectively. Of course, second order (and even more accurate) temporal implementations would be possible (see, e.g., the excellent Rider and Kothe [9] see in particular their page 118). This will be the subject of forthcoming analyses where some possible variations and improvements of the present method will be discussed and elucidated in the framework of level set and VOF methods. The present paper shows the ''bone structure'' of the technique. Further numerical studies in fact are in progress along these lines. The PLIC piecewise linear interface approximation used for the present computations, coupled with the second-order time integration scheme should result in a more accurate algorithm. This can be seen as an interesting and intriguing additional refinement of the present method.

6. Conclusions

A heretofore unseen mathematical model has been carefully developed for the case of macromolecular (protein) substances that are extremely complex physical-chemical systems whose properties may vary as a function of many environmental influences.

A novel volume tracking method specifically designed for the case under investigation has been introduced and applied to several 'typical' situations. This method, that eliminates the need for separate equations in each phase, by establishing conservation equations which are universally valid, allows a

fixed-grid solution to be undertaken and is therefore able to utilize standard solution procedures for the fluid flow and species equations directly, without resorting to mathematical manipulations and transformations (this feature, on the other hand, facilitates a parallel implementation of the code based on a grid partition strategy).

In the OCGVOF method, the 'phase field' ϕ is computed using incorporation kinetics at the surface of the solid mass, i.e., it is computed taking into account the phenomenon of addition/incorporation of solute molecules (building blocks or growth units) to the crystal. The kinetic conditions in fact are coupled to the exchange mass flux at the interface and lead to the introduction of a group of differential equations for the protein concentration at the crystal surface and the evolution of the solid mass displacement. The growth velocity is not directly imposed but it results from internal conditions related to solute transport.

The analogies and differences among this method and previous 'moving boundary' methods have been pointed out.

For a realistic description, anisotropy in interface kinetics has been considered. This situation occurs for crystalline proteins which have high anisotropy (preferred orientations) in either their surface energy or atomic attachment kinetics. The method has been proved to be able to predict shape morphology instabilities (i.e., habit change) according to the (experimentally found) dependence of the face growth rates on the level of supersaturation (in the case of attachment kinetics dominant in limiting crystal growth rate) as well as the onset of surface depressions due to diffusive and/or convective effects in the case of incorporation kinetics and mass transport competitive in limiting the growth rate.

For this case an analysis of the distribution of the local growth rate along the sides of the crystal has been carried out. The growth rate has been found to be non-uniform across the crystal faces (growth rate always lower at the centre than at the corner) irrespective of the prevailing transport (diffusive or convective) mode with the asymmetry more evident however for the convective case.

This follows since the 'steepness' of the concentration gradient determines the rate of incorporation of the solute into the crystal (the steepness being maximum around the corners for the diffusive case). The larger asymmetry in the case of presence of convection has been explained according to the fact that around the corners the convective flows are very strong and tend to increase the steepness of the concentration gradient there.

For the first time the (still unknown in literature and contradictory) relative importance of surface attachment kinetics and mass transport in liquid phase has been discussed through the computation of the 'quantitative' parameter γ. This parameter is increased if the dimensions of the system under investigations are increased and for a fixed system it is decreased by the effect of convection.

This trend has been explained according to the fact that, if the dimensions of the system are increased, a high time is required to transport available protein (in solute phase) from far regions (i.e., the frontier of the reactor) towards the crystal surface whereas, if convection enhances mass transport, this time is reduced.

The effect of typical microgravity conditions has been investigated. A concentration depletion zone of considerable width develops about the growing crystal. Such solutal boundary layers are responsible for the onset of convection under the effect of residual gravity acceleration. The less dense layer adjacent to the growth interface in fact tends to rise, causing a convective flow to occur about the growing crystal which considerably alters the boundary layer conditions. Convection in fact strongly changes the (diffusive) concentration distribution about the crystal. Depending on its strength and direction with respect to the crystal surface, convection has been observed to modify growth rates and morphological stability with respect to diffusion controlled (bulk) transport.

The effect of convection on the macroscopic growth rate has been proved to be not trivial. It is strictly coupled to the effect of the 'finite' size of the reactor where crystallization is carried out.

Convection enhances mass transport in liquid phase thus increasing the rate of incorporation (growth rate) of the solute into the crystal, but at the same time, it can lead to a more rapid decrease of the finite amount of protein available in solute phase and thus to a decrease of the macroscopic growth rate.

An important parameter is the relative direction of the residual gravity vector relative to the different facets, which induces varying conditions for each facet. The isotropic solutal field around a crystal is deformed by gravity. This leads to flow parallel to the vertical facets and to pluming on the upper horizontal one. Different facets, therefore, grow with different growth rates.

The convection effect results in higher local growth rate near the surface where the flow is incoming and lower local growth rate near the surface where the flow is outgoing. This clearly demonstrates that orientation-dependent growth may occur even if the dependence of the kinetic coefficients on the orientation of the faces is neglected. In the case of surface attachment kinetics and transport in liquid phase competitive in limiting the growth rate, the present simulations show that the growth rate is strongly influenced by the mass transport in liquid phase and g-orientation-dependent growth occurs.

The role of the changes in the size of the crystallization sample in determining the intensity of the convective field (the magnitude of the flow, in fact, is directly proportional to the size of the face upon which it is being generated) and its structure (the increasing size of the crystal leads to a confinement of the convective cell) has been pointed out.

Many investigators found that growth was limited by surface kinetics alone. The present results have shown that claims that 'the role' of mass transport in liquid phase across the depletion layer can be eliminated are fluid-dynamically unsupportable. Crystal growth rates have to be considered in terms of both mass transport and attachment kinetics. The simulations, however, confirm that for protein crystals which grow relatively slowly and for typical dimensions of the reactors used for growth (of the order of few millimetres or centimetres), mass transport in liquid phase, dependent primarily on physical forces and movements in the solution phase, is almost certainly the less important of the two (for all the cases investigated in fact $\gamma < 0.4$).

A powerful mathematical tool (OCGVOF) and some information heretofore poorly understood by organic crystals growers have been made available for the scientific community to help the investigators to discern the interrelations among the various parameters under one's control (that are not independent of one another) and to elaborate rational guidelines relating to physical factors that can increase the probability of success in crystallizing protein substances. Further investigation is needed for parametric analyses of the effects described above.

Acknowledgements

This work has been supported by ASI (Italian Space Agency) and ESA (European Space Agency). The author would like to thank Dr. L. Carotenuto (MARS) for some helpful discussions and the Reviewers for the very constructive comments and suggestions.

References

[1] S.R. Coriell, A.A. Chernov, B.T. Murray, G.B. McFadden, Step bunching: generalized kinetics, J. Cryst. Growth 183 (1998) 669.
[2] A. Monaco, F. Rosenberger, Growth and etching kinetics of tetragonal lysozyme, J. Cryst. Growth 129 (1993) 465.
[3] P.G. Vekilov, A.A. Chernov, in: H. Ehrenreich, F. Spaepen (Eds.), The Physics of Protein Crystallization, Solid State Physics, vol. 57, Academic Press, Amsterdam, 2002, pp. 1–147.
[4] F. Otàlora, M.L. Novella, J.A. Gavira, B.R. Thomas, J.M. Garcìa-Ruiz, Experimental evidence for the stability of the depletion zone around a growing protein crystal under microgravity, Acta Cryst. D 57 (2001) 412.
[5] H. Lin, F. Rosenberger, J.I.D. Alexander, A. Nadarajah, Convective–diffusive transport in protein crystal growth, J. Cryst. Growth 151 (1995) 153.
[6] M.L. Pusey, R.S. Snyder, R. Naumann, Protein crystal growth: growth kinetics for tetragonal lysozyme crystals, J. Biol. Chem. 261 (14) (1986) 6524.
[7] D.S. Noh, Y. Koh, I.S. Kang, Numerical solutions for shape evolution of a particle growing in axisymmetric flows of supersaturated solution, J. Cryst. Growth 183 (1998) 427.

[8] F.H. Harlow, J.E. Welch, Numerical calculation of time-dependent viscous incompressible flow with free surface, Phys. Fluids 8 (1965) 2182.
[9] W.J. Rider, D.B. Kothe, Reconstructing volume tracking, J. Comput. Phys. 141 (1998) 112.
[10] C.W. Hirt, B.D. Nichols, Volume of fluid (VOF) method for the dynamics of free boundaries, J. Comput. Phys. 39 (1981) 201.
[11] S. Osher, J.A. Sethian, Fronts propagating with curvature-dependent speed: Algorithms based on Hamilton–Jacobi formulations, J. Comput. Phys. 79 (1988) 12.
[12] J.U. Brackbill, D.B. Kothe, C. Zemach, A continuum method for modeling surface tension, J. Comput. Phys. 100 (2) (1992) 335.
[13] O.S. Unverdi, G. Tryggvason, A front tracking method for viscous incompressible flows, J. Comput. Phys. 100 (1992) 25.
[14] M. Sussman, P. Smereka, S. Osher, A level set approach for computing solutions to incompressible two-phase flow, J. Comput. Phys. 114 (1994) 146.
[15] D. Gueyffier, J. Li, A. Nadim, S. Scardovelli, S. Zaleski, Volume of Fluid interface tracking with smoothed surface stress methods for three-dimensional flows, J. Comput. Phys. 152 (1999) 423.
[16] S. Osher, R. Fedkiw, The Level Set Method and Dynamic Implicit Surfaces, Springer, New York, 2002.
[17] J. Sethian, Level Set Methods and Fast Marching Methods, Cambridge University Press, Cambridge, 1999.
[18] E. Ory, H. Yuan, A. Prosperetti, S. Popinet, S. Zaleski, Growth and collapse of a vapor bubble in a narrow tube, Phys. Fluids 12 (2000) 1268.
[19] M.R. Nobari, Y.J. Yan, G. Tryggvason, Head-on collision of drops-a numerical investigation, Phys. Fluids 8 (1996) 29.
[20] E. Bassano, Numerical simulation of thermo-solutal-capillary migration of a dissolving drop in a cavity, Int. J. Numer. Meth. Fluids 41 (2003) 765.
[21] V.R. Voller, C. Prakash, A fixed grid numerical modelling methodology for convection-diffusion mushy region phase-change problems, Int. J. Heat Mass Transfer 30 (8) (1987) 1709.
[22] W.D. Bennon, F.P. Incropera, A continuum model for momentum, heat and species transport in binary solid–liquid phase change systems-I. Model formulation, Int. J. Heat Mass Transfer 30 (10) (1987) 2161.
[23] W.D. Bennon, F.P. Incropera, A continuum model for momentum, heat and species transport in binary solid–liquid phase change systems-II. Application to solidification in a rectangular cavity, Int. J. Heat Mass Transfer 30 (10) (1987) 2171.
[24] A.D. Brent, V.R. Voller, J. Reid, Enthalpy–porosity technique for modelling convection–diffusion phase change: application to the melting of a pure metal, Num. Heat Transf. 13 (1988) 297.
[25] H.S. Udaykumar, R. Mittal, W. Shyy, Computation of solid–liquid phase fronts in the sharp interface limit on fixed grids, J. Comput. Phys. 153 (2) (1999) 535.
[26] C. Beckermann, H.-J. Diepers, I. Steinbach, A. Karma, X. Tong, Modeling melt convection in phase-field simulations of solidification, J. Comput. Phys. 154 (2) (1999) 468.
[27] C.W. Lan, M.C. Liang, Multigrid methods for incompressible heat flow problems with an unknown interface, J. Comput. Phys. 152 (1) (1999) 55.
[28] D. Knoll, D. Kothe, B. Lally, A new nonlinear solution method for phase change problems, Num. Heat Transfer Part B 35 (4) (1999) 439.
[29] M. Lappa, R. Savino, 3D analysis of crystal/melt interface shape and Marangoni flow instability in solidifying liquid bridges, J. Comput. Phys. 180 (2002) 751.
[30] C.W. Lan, C.C. Liu, et al., An adaptive finite volume method for incompressible heat flow problems in solidification, J. Comput. Phys. 178 (2) (2002) 464.
[31] D.B. Kothe, R.C. Ferrell, J.A. Turner, S.J. Mosso, A high resolution finite volume method for efficient parallel simulation of casting processes on unstructured meshes, presented at the 8th SIAM Conference on Parallel Processing for Scientific Computing, Minneapolis, MN, March 14–17, 1997.
[32] A.V. Reddy, D.B. Kothe, C. Beckermann, R.C. Ferrell, K.L. Lam, High resolution finite volume parallel simulations of mould filling and binary alloy solidification on unstructured 3-D meshes, in: J. Beech, H. Jones (Eds.), Proceedings of the Fourth Decennial International Conference on Solidification Processing, The University of Sheffield, UK, July 7–10, 1997, pp. 83–87.
[33] S. Chen, B. Merriman, S. Osher, P. Smereka, A simple level set method for solving Stefan problems, J. Comput. Phys. 135 (1) (1997) 8.
[34] Y.T. Kim, N. Goldenfeld, J. Dantzig, Computation of dendritic microstructures using a level set method, Phys. Rev. E 62 (2000) 2471.
[35] A. McPherson, Current approaches to macromolecular crystallization, Eur. J. Biochem. 189 (1990) 1.
[36] Yu.G. Kuznetsov, A.J. Malkin, A. Greenwood, A. McPherson, Interferometric studies of growth kinetics and surface morphology in macromolecular crystal growth: canavalin, thaumatin and turnip yellow mosaic virus, J. Struct. Biol. 114 (1995) 184.
[37] F. Rosenberger, Inorganic and protein crystal growth: similarities and differences, J. Cryst. Growth 76 (1986) 618.
[38] C.W. Boistelle, J.P. Astier, Crystallization mechanisms in solution, J. Cryst. Growth 90 (1988) 14.
[39] P.G. Vekilov, J. Iwan, D. Alexander, F. Rosenberger, Non-linear response of layer growth dynamics in the mixed kinetics-bulk transport regime, Phys. Rev. E 54 (6) (1996) 6650.

[40] M. Lappa, D. Castagnolo, L. Carotenuto, Sensitivity of the non-linear dynamics of Lysozyme "Liesegang Rings" to small asymmetries, Physica A 314 (1–4) (2002) 623.
[41] M. Lappa, D. Castagnolo, Complex dynamics of rhythmic patterns and sedimentation of organic crystals: a new numerical approach, Num. Heat Transfer B 43 (4) (2002) 373.
[42] R. Monti, R. Savino, M. Lappa, S. Tempesta, Behaviour of drops in contact with liquid surfaces at non-wetting conditions, Phys. Fluids 10 (11) (1998) 2786.
[43] R. Savino, D. Paterna, M. Lappa, Marangoni floatation of liquid droplets, J. Fluid Mech. 479 (2003) 307.
[44] M. Lappa, Three-dimensional numerical simulation of Marangoni flow instabilities in floating zones laterally heated by an equatorial ring, Phys. Fluids 15 (3) (2003) 776.
[45] M. Lappa, Strategies for parallelizing the three-dimensional Navier–Stokes equations on the Cray T3E, in: M. Voli (Ed.), Science and Supercomputing at CINECA, Bologna, vol. 11, 1997, p. 326.
[46] M. Lappa, R. Savino, Parallel solution of three-dimensional Marangoni flow in liquid bridges, Int. J. Num. Meth. Fluids 31 (1999) 911.
[47] M. Lappa, The growth and the fluid-dynamics of protein crystals and soft organic tissues: models and simulations, similarities and differences, J. Theoret. Biol. (2003), accepted for publication, in press.
[48] F. Otàlora, J.M. Garcìa-Ruiz, Crystal growth studies in microgravity with the APCF: Computer simulation and transport dynamics, J. Cryst. Growth 182 (1997) 141.
[49] R. Monti, R. Savino, M. Lappa, Microgravity sensitivity of typical fluid physics experiment, presented at the 17th Microgravity Measurements Group Meeting, Cleveland, OH, March 1998, published in the meeting proceedings in NASA CP-1998-208414, 23 (1998) 1.
[50] R. Monti, R. Savino, M. Lappa, On the convective disturbances induced by *g*-jitter on the space station, Acta Astronaut. 48 (5–12) (2001) 603.
[51] R. Savino, M. Lappa, Assessment of the thermovibrational theory: application to *g*-jitter on the Space-station, J. Spacecraft Rockets 40 (2) (2003) 201.
[52] M. Lappa, L. Carotenuto, Effect of convective disturbances induced by *g*-jitter on the periodic precipitation of lysozyme, Microgravity Science & Technology XIV/2 (accepted, in the press, scheduled for July 2003).
[53] C. Piccolo, M. Lappa, A. Tortora, L. Carotenuto, Non-linear behaviour of lysozyme crystallization, Phys. A 314(1–4) (2002) 636.
[54] M. Lappa, C. Piccolo, L. Carotenuto, Numerical and experimental analysis of periodic patterns and sedimentation of lysozyme, J. Cryst. Growth 254 (3–4) (2003) 469.
[55] L. Carotenuto, C. Piccolo, D. Castagnolo, M. Lappa, J.M. Garcìa-Ruiz, Experimental observations and numerical modelling of diffusion-driven crystallisation processes, Acta Cryst. D 58 (2002) 1628.